MEASURED VERSUS MODELED OZONE DRY DEPOSITION

by
L.N. Ganzeveld

Measured versus modeled Ozone dry deposition.

A comparison between the measured ozone deposition velocity at the Pawnee grasslands in Colorado and the ozone deposition velocity derived by an inferential dry deposition model.

By

L.N Ganzeveld[1]

Presentation of a study carried out during a 6-month internship, contract number 28-C2-590

USDA/Forest Service
Rocky Mountain Forest and Range Experiment Station
240 West Prospect Street
Fort Collins, Co 80526, USA

[1] Wageningen Agricultural University
Department of Air Pollution
PO BOX 8129
6700 EV Wageningen
The Netherlands

August 1992

Preface

This paper is the presentation of the results of a six-month internship at the Rocky Mountain Forest and Range Experiment Station in Fort Collins. This internship is one of the required parts of the study program of the Department of Air Pollution of the Wageningen Agricultural University. Besides the experience of working on a specific issue of the air pollution, there is also the opportunity to get experience with all the other aspects of the kind of work that I can expect to do in the future after my graduation. Last six months have given me a good foundation to determine in which direction I would like to go in the future. I really would like to emphasis this major advantage of such an internship (in a foreign country), besides of the course the personal experience of meeting a lot of new friens and living in a state as Colorado with its great landscape.

Abstract

Increasing concentrations of ozone in the troposphere and, related to that, an increase of dry deposition of ozone, is considered an important current environmental problem. In this paper, the performance of a Dry Deposition Inferential Model (DDIM), developed by the Air Resources Laboratory Atmospheric Turbulence and Diffusion Division (ATDD) of NOAA (Oakridge, TN), is presented for the dry deposition of ozone. The modeled ozone deposition velocity (V_dO_3) is compared with the deposition velocity determined from measurements which are being carried out on the Pawnee Grasslands in Colorado by the Rocky Mountain Forest and Range Experiment Station (RMFRES, Fort Collins, Co) and NOAA. For the comparison, the data of six weeks in the summer of 1989 are used.
The DDIM is a model in which the deposition of the trace gas is described by a resistance analog. The V_d is defined as:

$$(3.1.1) \qquad V_d = \frac{1}{r_a + r_b + R_c}$$

The aerodynamic resistance r_a is determined in the model using the sigma theta method:

$$(3.2.1) \qquad r_a = \frac{c_v^2}{\sigma_\theta^2 \, \overline{u}}$$

For the Pawnee-site, c_v has a value of 2.03 for stable conditions, 1.79 for neutral conditions and 2.64 for unstable conditions. However, based on the difficulty to determine the stability out of the small selection of input data, it is assumed that c_v has a value of 2.64 for unstable conditions and 2 for neutral and stable conditions. The criterion used to determine the stability class is the global radiation, R_G (> 75 W m^{-2}, then unstable). The correlation between r_a (z/L) and r_a (σ_θ) is small, especially under stable conditions.
The surface resistance R_c is the combined resistance of the soil ($r_{sl}O_3$) and the canopy (R_{fol}). In the DDIM the canopy is described as a multi-layer model by dividing it in twenty-one layers. For every layer, the free-stream velocity is determined and also the distribution of diffuse and direct photo synthetically radiation. R_{fol} is the combined resistance of r_b, the boundary layer resistance, r_{cut}, the cuticular resistance (parallel) and R_s, the stomatal resistance. R_s is the sum of the stomatal resistance of the shaded and unshaded leaves.
The measured dry deposition velocity at the Pawnee-site is determined out of the ozone flux which is measured using the eddy correlation technique. Corrections were made in order to correct for errors introduced in the measured flux due to for example instrumentation separation and fluxes of heat and water vapor. These corrected measured fluxes are used for the comparison. Information concerning the leaf area index, needed to run the model, is based on measurements carried out in 1988 and 1989 at the Pawnee-site.
A sensitivity analysis indicates that V_dO_3 is most sensitive for changes in r_a, $r_{sl}O_3$, the minimal stomatal resistance r_{smin}, and the LAI. A decrease of $r_{sl}O_3$ causes an increase in V_dO_3 for as well the night as in the day-time. An decrease of r_{smin} and increase of LAI cause an increase of the amplitude of V_dO_3, since these quantities only play an role in determining V_dO_3 in the day-time. The $r_{sl}O_3$, determined out of the night data for all the five weeks used for the comparison, are all significantly larger compared with the value of 170 s m^{-1} found by Massman (1992). Assuming that there is not a diurnal cycle in $r_{sl}O_3$ and r_{smin} = 50 s m^{-1}, there is reasonable agreement between the model-derived and corrected measured V_dO_3 for Julian day 157 through 164. For the other periods there is disagreement, especially concerning the fluctuations. This is caused by the combination of large $r_{sl}O_3$ values and a bad estimate of r_a by the sigma theta method, especially during the nights. If it is assumed that there is a diurnal cycle in $r_{sl}O_3$ and r_{smin} = 125 s m^{-1}, a value in better agreement with values found in previous research, it is possible to estimate the magnitude of the amplitude of this diurnal cycle. However, runs of the model using two different

values for $r_{sl}O_3$ for in the night- and day-time don't cause an improvement of the model concerning the prediction of the fluctuations. Only an impact on the absolute level of V_dO_3 can be seen.

Contents

1. Introduction

Increasing concentrations of ozone in the troposphere and, related to that, an increase of dry deposition of ozone, is considered an important current environmental problem. Knowledge about all the aspects of this environmental problem is one of the basic requirements in justifying environmental policy. To get more insight in the controlling factors of the dry deposition process, extensive measurement campaigns are being carried out to determine the dry deposition of ozone. Yet, measurement campaigns have the disadvantage that their results are only valid for the specific circumstances of the measurement site since the exchange of air trace gas with the surface is effected by a wide variety of meteorological, chemical and biological processes (Hicks, B.B. and Matt, D.R, 1987). Other relationships must be used for another location with a different type of vegetation and another fetch in order to describe the dry deposition.

In general, micrometeorological methods are sufficiently complicated that routine application in a monitoring network is not yet practical (Hicks, B.B. et.al., 1987). A way to deal with this problem is to model the dry deposition in order to quantify it for any location, using data that can be collected in a simplified way compared with the usually required intensive micrometeorological methods.

In this paper, the performance of a Dry Deposition Inferential Model (DDIM), developed by the Air Resources Laboratory Atmospheric Turbulence and Diffusion Division (ATDD) of NOAA (Oakridge, TN), is presented for the dry deposition of ozone. The term inferential is based on the determination of the deposition velocity, using a model that needs some specifically selected controlling variables, an essentially inferential method (Hicks, B.B. et.al. 1987). The modeled ozone deposition velocity is compared with the deposition velocity determined from measurements which are being carried out on the Pawnee Grasslands in Colorado by the Rocky Mountain Forest and Range Experiment Station (RMFRES, Fort Collins, Co) and NOAA.

2. Objectives

The objectives of this study are:
1) To investigate possible systematic differences between the measured and model derived deposition velocity and, if present, the causes of this systematic differences. An important aspect of this investigation is a sensitivity analysis of the model derived deposition velocity for different quantities. The results of the sensitivity analysis will indicate which quantities need the most attention for improvement of the model;
2) To investigate the performance of NOAA's DDIM by comparing the model-derived ozone deposition velocity with the observed deposition velocity at the Pawnee site. From this, conclusions can be drawn about how accurately the model simulates the total amount of ozone that is deposited over a longer period of time on the surface.

3. Description of the DDIM

3.1 Introduction

The DDIM is a model in which the deposition of the trace gas is described by a resistance analog. The V_d is defined as:

$$(3.1.1) \qquad V_d = \frac{1}{r_a + r_b + R_c}$$

where V_d is the deposition velocity (in m s^{-1} or cm s^{-1}), r_a is the aerodynamic resistance, r_b the quasi-laminar boundary layer resistance and R_c is the surface resistance. In this study, a positive value of V_d represents downward transport. r_a is wholly determined by atmospheric properties (predominantly by turbulent exchange), r_b accounts for the fact that trace gas transfer in the vicinity of receptor surfaces is affected by the molecular diffusivity. R_c combines the consequences of all uptake processes involving individual elements of the surface (vegetation and soil) into a single number that is characteristic of the trace gas in question and the surface at the site under consideration (Hicks, B.B. et.al. 1987). The definition of V_d given by equation 3.1.1 is a basic form of the resistance analog. The model uses a more specific form in which the surface resistance R_c is defined by the combination of the soil resistance r_{sl}, r_b and r_c, the canopy resistance. This specific form of equation 3.1.1 is based on the approach of the canopy describing it by a multi-layer model. So equation 3.1.1 can be rewritten to a definition in which only the r_a and R_c are used. Details concerning the specific determination of the R_c can be found in paragraph 3.3. The calculation of r_b is also presented in this paragraph because of its determination on canopy scale. The determination of r_a is presented in paragraph 3.2.

3.2 The aerodynamic resistance r_a

The aerodynamic resistance is determined in the model using the sigma theta method. r_a is defined by:

$$(3.2.1) \qquad r_a = \frac{c_v^2}{\sigma_\theta^2 \, \overline{u}}$$

where c_v is a parameter dependent on the atmospheric stability and on the boundary layer height z_i. σ_θ is the deviation of the wind direction and is defined by σ_v/u where u is the average windspeed. c_v Is assumed to have a value of 2 for neutral and stable conditions and 3 for unstable conditions (Hicks, B.B. et.al. 1987). Erisman and Duyzer determined values for c_v based on the results of measurements over heathland in the Netherlands. They found values for c_v that range from 1.79 (± 0.83) for stable conditions ($z/L > 0.02$ where z/L is a dimensionless stability parameter with z the measurement height and L the Monin Obukhov length) to 1.98 (± 0.33) for neutral ($-0.02 < z/L < 0.02$) and 1.88 (± 0.43) for unstable conditions ($z/L < -0.02$) (standard deviation in parenthesis) (Erisman, J. and Duyzer, J. 1991). Massman determined values for c_v based on data that were collected on sites covered with grapes and cotton in California. The results are presented in table 3.2 (Massman, W.J, personal communication 1992).

Table 3.2: c_v values with the standard error of the estimate of c_v in parenthesis and the number of data N in the third column.

Grape data:

stability class	value	N
z/L >= 0.02 (± 0.01) 631	c_v = 1.64 (± 0.01)	631
-0.02 < z/L < 0.02	c_v = 1.79 (± 0.02)	51
z/L <= -0.02	c_v = 1.62 (± 0.02)	438

Cotton data:

z/L > 0.02	c_v = 1.49 (± 0.03)	362
-0.02 < z/L < 0.02	c_v = 1.88 (± 0.07)	212
z/L <= -0.02	c_v = 1.89 (± 0.03)	453

For the Pawnee-site, c_v has a value of; 2.03 (± 0.46) for stable, 1.79 (± 0.12) for neutral and 2.64 (± 0.35) for unstable conditions (standard deviation in parenthesis). c_v is calculated using:

$$(3.2.2) \qquad c_v^2 = \frac{\sigma_\theta^2}{\kappa^2} \left[\ln\left(\frac{z}{z_0}\right) - \Psi_m\left(\frac{z}{L}\right)\right] \left[\ln\left(\frac{z}{z_{0C}}\right) - \Psi_C\left(\frac{z}{L}\right)\right]$$

where κ is Von Karman constant (0.40), z_0 and z_{0C} are respectively the surface roughness length for momentum (0.018 m) and mass and Ψ_m and Ψ_C are atmospheric stability influence functions for momentum and mass. Based on the Monin-Obukhov similarity theory in which it is assumed that mass is transported by atmospheric turbulence in a manner similar to heat, the Ψ_C can be replaced by Ψ_H, the stability influence function for heat. It is also assumed that the z_{0C} can be replaced by z_0. This replacement does not introduce a significant error. The same thresholds for z/L as used by Erisman and Duyzer are used for the c_v determination.
There is a lot of scatter in the c_v values of the Pawnee site even after a mere selection of the data as is shown in figure 3.2.1a and b. The criterion used for this selection is: $d\sigma_\theta/dt$, the change in σ_θ in order to filter out nonstationnary conditions ($|d\sigma_\theta/dt| < 0.06$ rad 30 minutes^{-1}). Also the 75% and 25% values of c_v are used to delete the most extreme values for unstable and neutral conditions and only the 75% for stable conditions (not a normal distribution). A T-test suggests that the value of 2.64 for unstable conditions is significantly different than 3 for a confidence level of 0.005. For stable conditions there is not a significant difference. For neutral conditions the T-test indicates that the value of 1.79 is significantly different than the reference value 2 for a confidence level of 0.005.

The figures presented here, especially those found by Erisman and Duyzer (Erisman, J. and Duyzer, J. 1991) and Massman (Massman, W.J. personal communication 1992), indicate that the c_v values are lower than previously found in other related literature. These results might be due to the fact that the kind of vegetation can induce a roughness sublayer at the level of the measurement equipment, resulting in a larger u_* and lower c_v values (Massman, W.J., personal communication 1992).

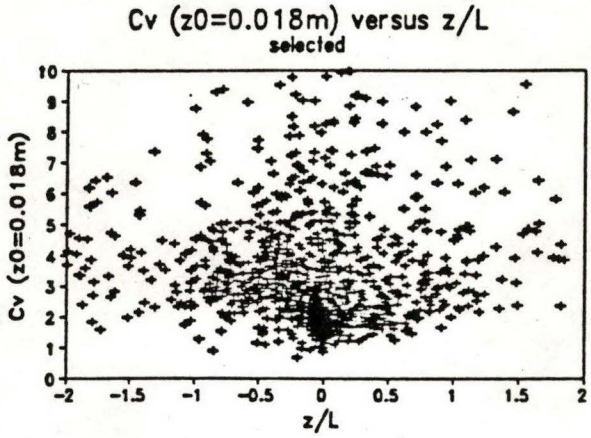

Figure 3.2.1a.--c_v for z_0 = 0.018 m versus z/L, the unselected data.

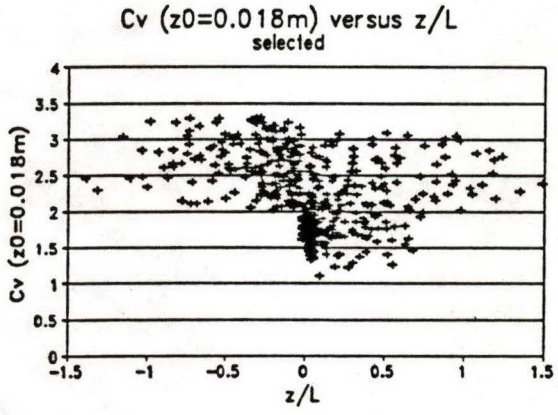

Figure 3.2.1b.--The same as in figure 3.2.1a for the selected data.

The model will normally be used to determine the V_d out of the small selection of input-data collected by a data collection system developed by NOAA. In that case there will only be data available concerning the global radiation R_G, the absolute ambient air temperature T_a, the average windspeed u, the deviation of the wind direction σ_θ, relative humidity rh and the canopy wetness. These selection of data can not be used for a direct z/L determination and so the value of c_v used to calculate r_a. The only way to determine z/L is to find a relationship between the measured quantities and z/L so that z/L can be estimated from the data. In the basic form of the model only R_G is used to make a distinction between unstable- and near-neutral conditions and stable conditions (threshold for z/L ± 0.02). Because of the more similar values for c_v for stable and neutral conditions a distinction between stable and neutral conditions and unstable conditions seems more useful (z/L ± -0.02). Attempts were made to improve the distinction by incorporating u, σ_θ and T_a in the determination of the stability. The strongest relationships can be found between z/L and R_G and z/L and σ_θ. At first, both variables were used to determine z/L but that

did not result in any improvement. Use of the new criteria, $R_G > 100$ W m^{-2} and $\sigma_\theta > 0.15$, causes more data to be selected in the stable class compared with the results using the old criteria, $R_G >$ 10 W m^{-2}. There is no improvement in the distinction between the two stability classes in the transition area around $z/L = \pm -0.02$. The only change actually made in order to get a more balanced distribution of the data around the transition area, is the increase of the threshold value of R_G from 10 to 75 W m^{-2}. The relative error in the separation of the data into the two stability classes is about 10% if only the R_G is used to define z/L.

The ultimate goal of defining a more accurate value of c_v is to improve the agreement between the measured and modelled V_d. Using c_v values of 2.64 instead of 3 for unstable and 2 for stable conditions can be justified based on the T-tests. For neutral conditions the T-test suggests that the value of 1.79 is significantly different than 2. However, because of the difficulty in making a clear distinction in the stability especially in the transition area, it is assumed that c_v has a value of 2 to incorporate neutral conditions in one group with the stable conditions. To find out if there is a significant impact on the V_d using the new value of c_v for unstable circumstances and the new threshold, $R_G > 75$ W m^{-2}, first $r_a(\sigma_\theta)$ is compared with $r_a(z/L)$ defined by:

$$(3.3.3) \qquad r_a = \frac{1}{u_* \kappa}\left[\ln\left(\frac{z}{z_0}\right) - \psi_H\left(\frac{z}{L}\right) + \psi_H\left(\frac{z_0}{L}\right)\right]$$

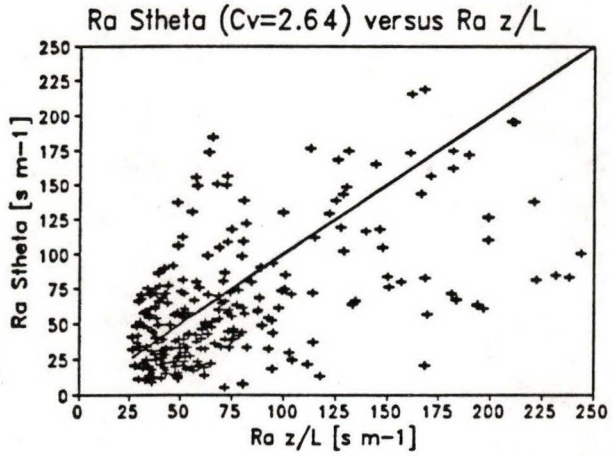

Figure 3.2.2a.--$r_a(\sigma_\theta)$ for $c_v = 2.64$ versus $r_a(z/L)$

Figure 3.2.2a shows the correlation between $r_a(\sigma_\theta)$ and $r_a(z/L)$ for the 24-hour data. In figure 3.2.2b and c the data collected in the day- and night-time are presented. To divide the 24 hour data in a day and night data set, a selection was made using the integrated canopy resistance R_{fol} (see 3.3) as selection criterion (day: $R_{fol} < 1000$ s m^{-1}, night: $R_{fol} > 1000$ s m^{-1}). It is obvious that the correlation between $r_a(z/L)$ and $r_a(\sigma_\theta)$ is small. During the night the correlation is worse compared with the data collected in the day-time. Only the graphs for $r_a(\sigma_\theta)$ using $c_v = 2.64$ versus $r_a(z/L)$ are presented here because the difference in correlation between $r_a(z/L)$ and $r_a(\sigma_\theta)$ using $c_v = 2.64$ or 3 is small. For $c_v = 2.64$ in the day-time, The R-squared was 0.08 and 0.06 for $c_v = 3$. The small correlation is probably caused by the scatter in σ_θ and the uncertainty in the

c_v value for the whole stability range. It may also be caused by the problem of determining z/L using the small selection of input-data. There must also be a contribution to the small correlation by the uncertainty in r_a (z/L), but it is assumed that this contribution is small. In figure 3.2.3 the residual value, r_a (σ_θ) - r_a (z/L), is plotted versus z/L. The largest residual values, about 250 s m^{-1}, can be found during stable conditions, which mostly occur during the night.

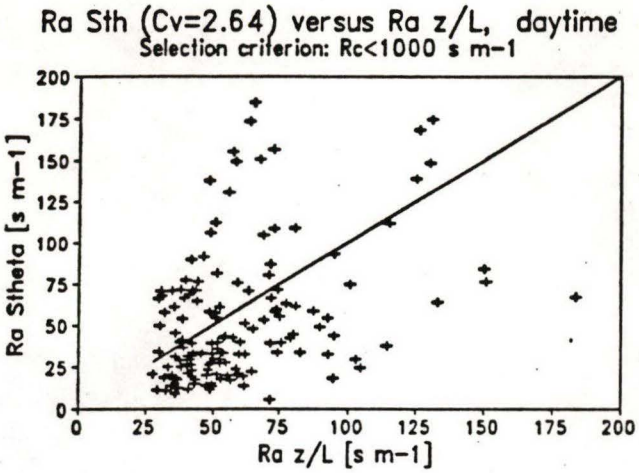

Figure 3.2.2b.--r_a (σ_θ) for c_v = 2.64 versus r_a (z/L) for the day-time.

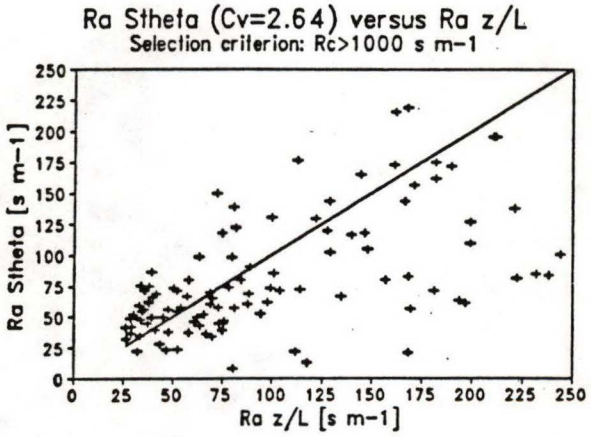

Figure 3.2.2c.--r_a (σ_θ) for c_v = 2.64 versus r_a (z/L) for the night-time.

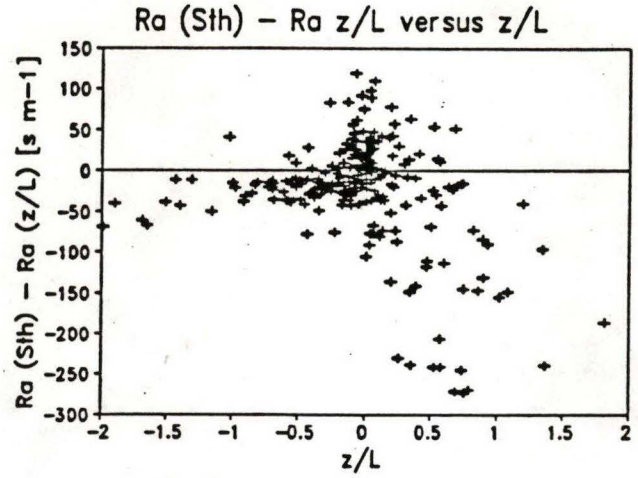

Figure 3.2.3.--$r_a(\sigma_\theta)$ - $r_a(z/L)$ versus z/L.

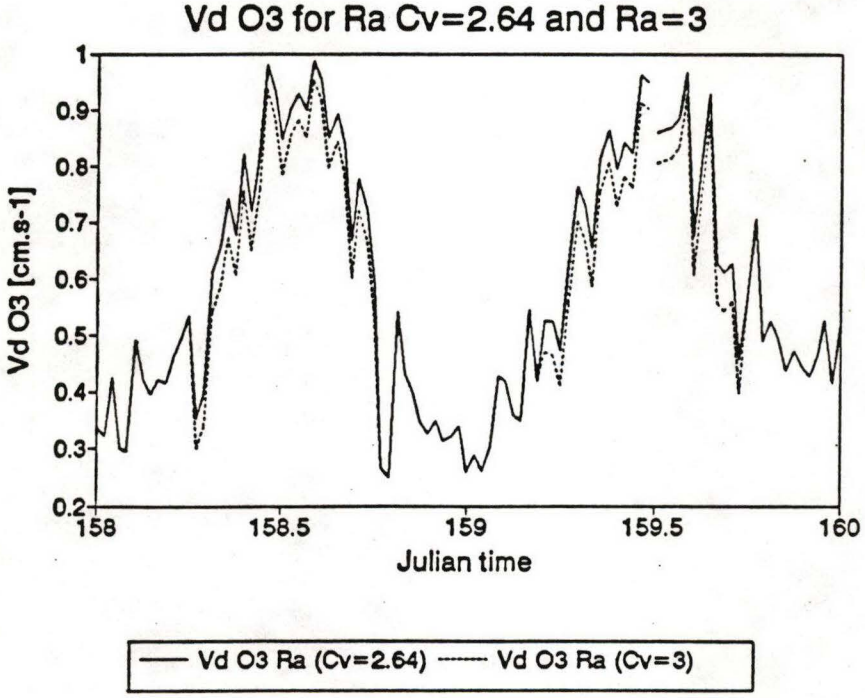

Figure 3.2.4.--V_dO_3 for $r_a(\sigma_\theta)$ determined using c_v = 2.64 and 3 for unstable conditions and c_v = 2 for neutral and stable conditions.

The difference in V_d for ozone using a c_v value of 2.64 and 3 is shown in figure 3.2.4. Only in the day-time is there a difference between the two curves with a maximum value of about 0.04 cm s^{-1}. The smallest absolute value of V_dO_3 where such a difference between the two curves can be seen is about 0.4 cm s^{-1}. So the maximum relative error in V_dO_3 will be about 10% (0.04/0.4*100%) using c_v = 3 instead of c_v = 2.64 for unstable conditions. The average V_dO_3 for

$c_v = 3$ is 0.59 cm s^{-1} and 0.62 cm s^{-1} for $c_v = 2.64$, so the relative change in V_dO_3 is ± 5%.

It seems that the overall influence on r_a caused by the change in the c_v values does not cause a significant change in the model-derived V_dO_3. This can only be seen in relation to the values of the other parameters that effect V_dO_3. However, in this study, a value of 2.64 is used for c_v when $R_G > 75$ W m^{-2} and $c_v = 2$ for $R_G < 75$ W m^{-2}.

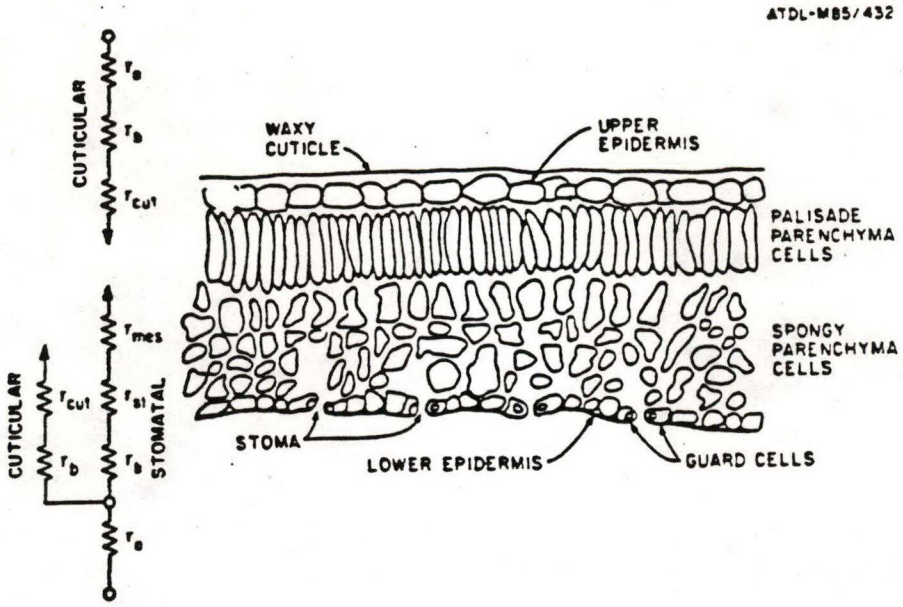

Figure 3.3.1.--A schematic illustration of the pathways and processes for transfer between air and plant tissue (following O'Dell et al., 1977).

3.3 The surface resistance R_c

The surface resistance R_c is the combined resistance of the soil and the canopy. In order to determine the canopy resistance r_c, there are different ways to model the canopy, for example the 'big leaf' approach in which no attempt is made to represent the detailed structure of the surface (Hicks, B.B. et al. 1987). In the DDIM the canopy is described as a multi-layer model by dividing it in twenty-one layers. This separation is needed because of the complex structure of some kinds of vegetation, such as forests. The complex structure can cause a significant change of the environment inside the canopy. There is for example the impact of the vegetation on the wind profile and the distribution of the diffuse and direct-beam radiation within the canopy. For the Pawnee site this separation into twenty-one layers is not essential because of the low canopy height and small leaf area index. Yet the model used for comparison still divides the canopy into twenty-one layers because it does not have a negative impact on the modeled $V_{dO}3$.

The canopy resistance r_c can be expressed in two different ways. The first definition of r_c is in terms of a biological resistance to transfer expressed as the effective resistances per unit area of foliar surface as is illustrated in figure 3.3.1 (Hicks, B.B. et al. 1987).
The resistance against transport from the atmosphere to the intercellular space in the plant tissue is the total of the boundary layer resistance r_b, the stomatal resistance r_s and the mesophyl

resistance r_{mes}, that are additive, and the parallel cuticular resistance r_{cut}:

$$(3.3.1) \qquad r_{ctot} = 1/[1/r_{cut} + 1/(r_b + r_s + r_{mes})]$$

The boundary layer resistance r_b is defined by:

$$(3.3.2) \qquad r_b = l/(v_s * Sh)$$

where l is the length of surface in the direction of the mean wind, v_s is the molecular diffusivity of the gas of interest (also denoted by D) and Sh is the Sherwood number. This equation can be rewritten to (Meyers T.P., 1987):

$$(3.3.3) \qquad r_b = \alpha\,(l/u)^{1/2}$$

with r_b in s m^{-1}, u is the free-stream velocity and α is assumed to have a value of 180. This value is based on the molecular diffusivity of SO_2 but this does not cause a significant error since the difference between the $v_s SO_2$ and $v_s SO_2$ is very small (0.12 versus 0.15 $mm^2\ s^{-1}$). In the model, a value of 0.07 m is used for l. The model's free-stream velocity is determined using Cionco's model in order to determine an exponential wind profile within the canopy over the whole range of twenty-one layers. (Cionco, R.M. 1972, cited in Hicks, B.B. et.al 1987). In figure 3.3.2 the r_b is presented for Julian day 157 through 165 for 1989 to give an impression of the fluctuations and absolute values of r_b.

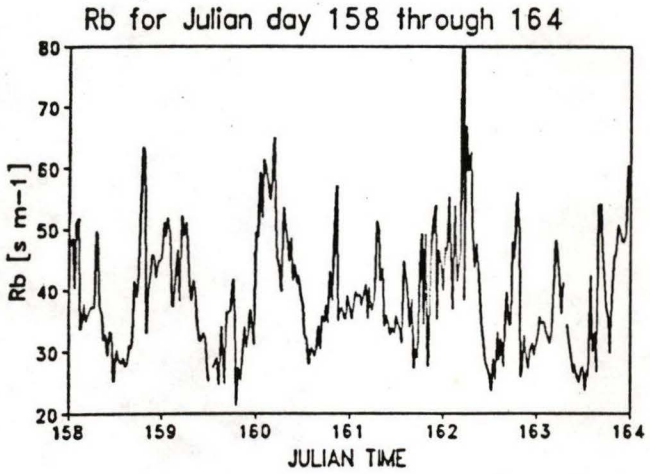

Figure 3.3.2.--r_b for Julian day 158 through 164.

The stomatal resistance r_s, is defined by:

$$(3.3.4) \qquad r_s = r_{smin}\,[1 + (b'/I_p)]\,/\,(f_e f_w f_T f_s)$$

where r_{smin} is the minimal stomatal resistance dependent on the plant species, I_p is the total diffuse and direct photosynthetically active radiation (W m^{-2}) and b' is a response coefficient equal to I_p on the leaf surface at 2 r_{smin} (Meyers, T.P. 1987). f_e, f_w, f_T and f_s are correction factors to make up for effects of humidity, water stress, temperature and difference between the molecular diffusivity of water vapor and the trace gas in question. The exact definition of these

correction factors can be found in Hicks, B.B. et al. 1987. The model's mesophyl resistance against ozone is assumed to be zero. The value of the cuticular resistance r_{cut} is related to the wetness of the canopy so that the r_{cut} decreases with an increasing canopy wetness.

The second definition of r_c is given by the first definition of r_{ctot} integrated to the total canopy resistance per unit horizontal area of the earth's surface. The link between these two definitions of r_c is the leaf area index LAI, as is shown by:

(3.3.5) $$R_{fol} = r_{ctot} / LAI$$

The upper case refers to the integrated value of a parameter (foliage scale). This relation is only valid for canopies with a small LAI. This relation could be used for the Pawnee grasslands but the model contains a more complex routine to determine the R_{fol}. This routine is based on the fact that in canopies with larger LAI, like forests, the stomatal resistance is strongly affected by shading caused by other foliage. To correct for this effect the LAI is partitioned into sunlit (L_s) and shaded portions (L_{sh}), for each of the twenty-one layers, by assuming a spherical leaf angle distribution (Hicks B.B. et al., 1987). The resulting R_{fol} is then defined by:

(3.3.6) $$R_{fol} = 1 / [1 / R_s + LAI / r_{cut}]$$

where

(3.3.7) $$R_s = 1 / [L_s / r_s (K I_{psun}) + L_{sh} / r_s (0.5 I_{pshade})]$$

K is the extinction coefficient (0.5/cos α and α is the zenith angle). The total PAR on the sunlit foliage and shaded foliage, I_{psun} and I_{pshade} respectively, are obtained by separating the total incoming global radiation into diffuse and beam components using the technique of Norman and Weiss (Norman J.M., Weiss A., 1985, cited in Hicks B.B. et al., 1987).

The determination of the resistance of the whole canopy including the ground, the surface resistance R_c, is finally completed by incorporating the soil resistance, $r_{sl}O_3$:

(3.3.9) $$R_c = 1 / [1 / R_{fol} + 1 / r_{sl}O_3]$$

The $r_{sl}O_3$ for the Pawnee site is determined by Massman. $r_{sl}O_3$ has a near-surface boundary layer component, r_u, of about 70 s m^{-1} and a intrinsic component which is associated with the destruction of ozone, r_i, of about 100 s m^{-1} (Massman, W.J. 1992). For the exact procedure used to determine the $r_{sl}O_3$, refer to Massman, W.J. 1992.

Finally using the definitions presented in this paragraph equation 3.2.1 in paragraph 3.1 can be rewritten to:

(3.3.9) $$V_d = \frac{1}{r_a + R_c}$$

4. Pawnee-site measurements

4.1 Eddy correlation measurements

The Pawnee measurement site, a research area of shortgrass prairie adjacent to and west of the Pawnee National Grasslands is 50 km northeast of Fort Collins, Co, at the Central Plains Experimental Range (CPER). The area is level, bordered on all sides by gently undulating plains, and is not near major ridges or bluffs that seriously influence the measurements.

On the Pawnee site, the deposition of ozone is determined using the eddy correlation technique. This method is based on the relation given in equation 4.1.1 that can be derived from the conservation equation for a scaler quantity that is transported through the atmospheric boundary layer.

$$F_c = \overline{w'c'} \qquad (4.1.1)$$

F_c is the vertical flux of the trace gas (ppb m s^{-1}) and w'c' is the covariance between the instantaneous deviation of the vertical windspeed, w', and the concentration, c'. The derivation is based on the following assumptions:

- horizontal uniformity
- steady state
- no sources and sinks.

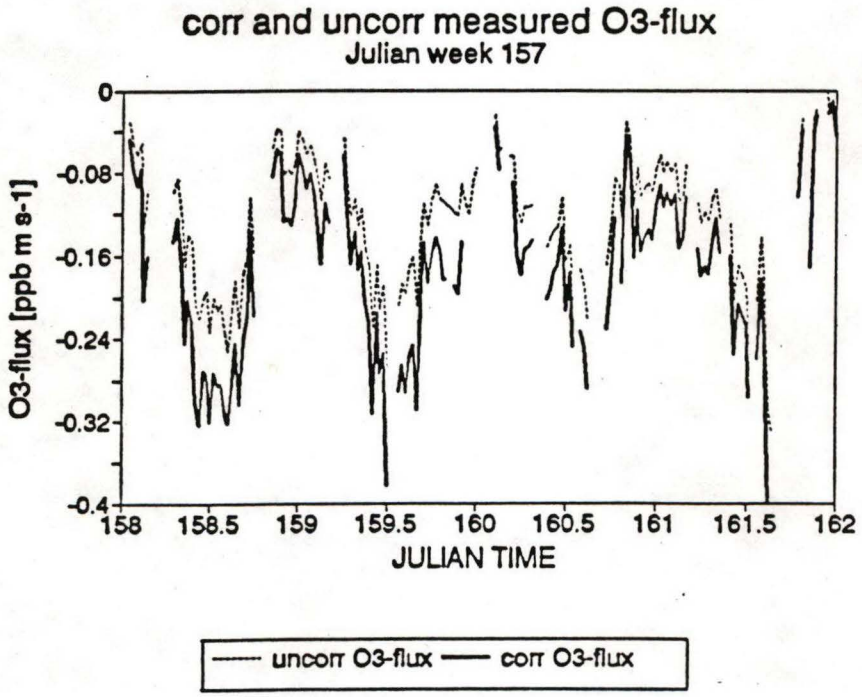

Figure 4.1.1.--The corrected- and uncorrected measured O_3-flux [ppb m s^{-1}].

Errors may be introduced in the measured flux due to fluxes of heat and water vapor, sensor limitations in size and response, instrumentation separation and mismatch, digitization noise, random uncorrelated noise, flow distortion effects and site inadequacies such as insufficient fetch and lack of surface uniformity (Zeller, K.F. et al. 1989). To prevent this errors, corrections are made in the measured fluxes. One disadvantage of these corrections is that the scatter in the corrected fluxes is larger than the scatter in the uncorrected fluxes. The 95% confidence interval for uncorrected ozone fluxes is 300% larger than the same interval for corrected fluxes. On the average, for both measurement heights (8- and 3 m) the corrected ozone fluxes were 1.34 times the uncorrected fluxes (Zeller K.F., 1990). Another disadvantage is that the flux corrections causes the rejection of a certain amount of data and so loss off information. The graphs for the uncorrected and corrected O_3-flux for Julian day 158 through 162 are shown in figure 4.1.1. The relation needed to compare the measured flux with the modeled deposition velocity is defined by:

$$(4.1.2) \qquad V_d = \frac{F_c}{\overline{c}}$$

where c is the average concentration of the trace gas on the measurement height (ppb or ppm). More details concerning the exact position of the site, the data collection system and the theory behind the flux corrections can be found in Zeller, K.F. et al. 1989.

4.2 The Leaf Area Index (LAI)

The vegetation at the measurement location is sparse with a total leaf area index of about 0.7. The surface is composed of about 2/3 live plant material and 1/3 dead plant material and bare soil (Hazlett D.L., 1992). The dominant vegetation on the Pawnee site is the Blue gramma grass (Bouteloua gracilis), a C_4 type of vegetation. Bouteloua gracilis-Agropyron Smithii (C_3) plant communities and Stipa Comata (C_3) are also present. The last is common and nearly a codominant vegetation in the immediate vicinity of the measurement tower (Zeller, K.F. et al. 1989). Cacti, Forbs and Shrubs were also present on the site but only in small amounts.

In 1988 and 1989, leaf area indices (LAI) measurements were carried out in order to find a relationship between the LAI and ozone flux. The LAI of old standing, live green, C_3 graminoids, and C_4 grasses was determined for ungrazed and grazed sites (Zeller, K.F. and Hazlett, D.L. 1989). The results of the measurements are used to estimate the values of the maximum LAI, and the contribution of the different kinds of vegetation to this maximum LAI defined by a percentage of maximum LAI. Both the grazed and the ungrazed LAI need to be incorporated in the estimate of the maximum LAI for the site. Although the measurement tower is positioned on a site covered with ungrazed vegetation, it can be expected that the grazed vegetation will have an impact on micro-climate above the ungrazed vegetation. This is based on the small area of the ungrazed site (4 ha.) and the fact that the ungrazed site is completely surrounded by a field covered with grazed vegetation. Table 4.2 shows the maximum LAI for the live green vegetation for both the grazed and ungrazed sites in the form of total-, C_3, C_4 LAI for 1988 and 1989 (Hazlett, D.L. 1992). The difference between total LAI and the sum of C_3 and C_4 is the contribution to the LAI by the Cacti, Forbs and Shrubs. Hazlett made a distinction in the LAI for the vegetation on a clay-loam site and a loam site. Table 4.2 shows the average LAI of both sites. The figures presented refer only to live green material. In addition to live green material, the canopy also contains old dead material from previous years and dead material from current growing season. Their contribution to the maximum LAI is not incorporated in the maximum LAI and percentages.

At the moment, there is little information available about the impact of the inactive (dead) vegetation on the deposition of ozone. Massman (1992) shows based on ozone deposition data obtained by eddy correlation over a surface dominated by dead grass in California, that the canopy resistance of the dead vegetation, r_{dead}, is likely to be less than 3000 s m^{-1} for the Pawnee site. This value is based on the surface resistance of the California site of 750 s m^{-1} for a canopy largely covered by dead grass. Incorporating the r_{dead} (parallel resistance with r_c) in the determination of $r_{sl}O_3$ results in a increase of $r_{sl}O_3$ from 170 to 180 s m^{-1} (standard error of the estimate ± 50 s m^{-1}) (Massman, W.J. 1992). Since V_dO_3 is basically controlled by the $r_{sl}O_3$ because of the larger values of the r_c and r_{dead} compared with $r_{sl}O_3$, and because $r_{sl}O_3$ does not change significantly by incorporating the r_{dead} in the total surface resistance, the impact of the dead vegetation on the V_dO_3 is small. Although the dead vegetation plays a small role in the active removal of ozone from the atmosphere, it can still have an impact on the ozone deposition caused by the contribution of the dead material in the height and density of the canopy. The dead material can, for example, cause increased shading of active leaves which in turn causes an increase in stomatal resistance. However, this probably is not relevant for the Pawnee site because of the small LAI and low canopy height. Even for the total LAI (green and dead material) shading effects can be neglected, and the impact of the vegetation on the windprofile is so small that no wind profile within the canopy needs to be determined.

Table 4.2.--The total-, C_4- and C_3 LAI [ratio] for the grazed and ungrazed sites at the Pawnee measurement site for 1988 and 1989. The values are the average LAI of the vegetation on the clay-loam and loam soils.

Green LAI	grazed 1988	grazed 1989	ungrazed 1988	ungrazed 1989
Total	0.36	0.42	0.41	0.54
C-4	0.24	0.31	0.26	0.38
C-3	0.08	0.04	0.08	0.08

In figure 4.2.1 a typical seasonal LAI pattern for the Pawnee grasslands is shown in the form of the seasonal LAI pattern of the Loam, grazed and ungrazed site.

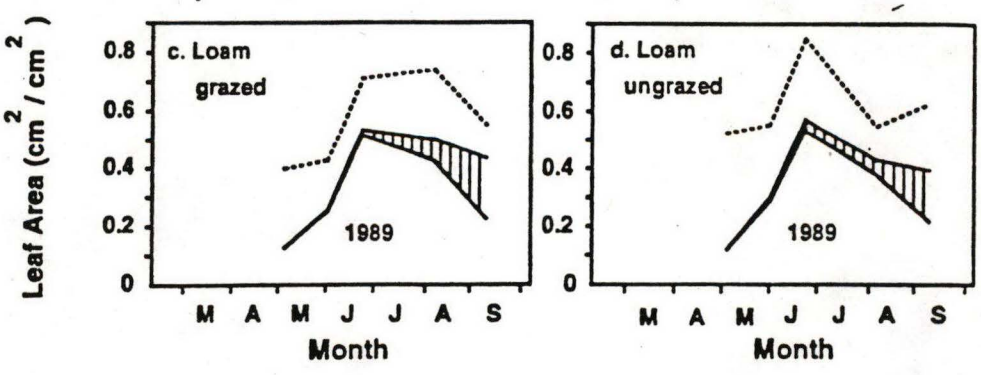

Figure 4.2.1.--Seasonal LAI patterns for the Loam, grazed and ungrazed site, 1989 (source Hazlett, D.L. 1992).

For the seasonal LAI patterns of the other sites and year, one must refer to Hazlett, D.L. (1992). The LAI of the live, current year green tissue increases from about 0.1 in the first week of May to a maximum of about 0.5 in the last week of June

5. Approach

To compare the measured and modeled ozone deposition velocities, two periods in 1989 are selected from the measurement data set. The first period is from May 16 through May 23 (Julian day 136 through 143) and the second period is from June 6 through July 11 (Julian day 157 through 192). These periods are selected based on the completeness and continuity of the quantities measured and the operating integrity of the overall data-collection system of the RMFRES measurements campaign (K.F. Zeller, 1990). As is already stated before, the RMFRES-equipment collected data on two different heights (3- and 8 m).
Besides the input-data of the RMFRES, other input-data concerning the precipitation, relative humidity, canopy wetness and net radiation, are needed. These data are collected by NOAA. Also data concerning the average windspeed, the standard deviation of the windspeed and wind direction are measured by NOAA on a height of 10 m. After a check of the a set, it appeared that this data set does not impose any restriction on the selected periods used for the comparison. If not stated differently, the RMFRES-data collected at 8m height are used to model V_dO_3

To achieve the first objective, to investigate the cause of any present systematic differences, different values for quantities like $r_{sl}O_3$, r_{smin} etc. are used, in order to investigate the sensitivity of V_dO_3 for these quantities. For the sensitivity research the data of Julian week 157 are used. Julian week represents here, and in the rest of the paper, the week starting with the Julian day given by the number. The results of this sensitivity research can be used as an indication as, which quantities need the most attention to decrease the systematic differences between the modeled and measured $V_{dO}3$. The improvement in the determination of r_a presented in paragraph 3.2 can for example only be seen in prospective of the sensitivity of the model for the other quantities.

To compare the model derived V_dO_3 and the measured V_dO_3, the model is run for the selected periods using the different input-data, of the RMFRES at a height of 3 m and 8 m. The data of both the measurement heights are used for the comparison in order to investigate the impact of the measurement height on the performance of the model. Also the data of NOAA collected at a height of 10 m are used to model the V_dO_3 in order to investigate the difference in V_dO_3 caused by using the NOAA data instead of the RMFRES-data. The measured and model-derived V_dO_3 are integrated over a whole week in order to investigate the performance of the model in predicting the total deposited ozone for a longer period.

In table 5.1, the default values of the quantities used to compare the modeled and measured are presented. Unless stated differently, these values are used to model the V_dO_3. The value of r_{smin} presented here, is the r_{smin} for H_2O. In the model, these value is used to determine the r_{smin} for O_3. The optimum, minimal and maximum temperature presented in the table are needed to determine the correction factor f_T used in equation 3.3.4. The values of these quantities are dependent on the kind of vegetation.

There are more quantities used in the model but these quantities have a constant value independent of the specific properties of the measurement location like the kind of vegetation. The choice for these constant values is related to a specific way of calculation of quantities like f_e and f_w. Especially in the sensitivity analysis, which is presented in the next chapter, it could be interesting to give attention to the impact of these quantities on the modeled V_dO_3. However, this study is restricted to the quantities mentioned in table 5.1.

Table 5.1.--Default values of the quantities used in the model

description, definition	value, units
maximum LAI:LAImax	0.5 ratio
soil resistance: $r_{s1}O_3$	170 $s\ m^{-1}$
minimal stomatal resistance: r_{smin}	50 $s\ m^{-1}$
light response coefficient: b'	50 $W\ m^{-1}$
optimum temperature: T_0	30 ^0C
maximum temperature: T_h	40 ^0C
minimum temperature: T_e	5 ^0C

The values of r_{smin}, b', T_0, T_h and T_e in table 4.1 are the characteristic values of Blue gramma grass. The r_{smin} of 50 $s\ m^{-1}$ (H_2O) for Bluegrass was found by Monson et al. (1986). The default values are used in this study since it is assumed that the whole canopy is formed by the Blue gramma grass. In the model there is the opportunity to separate the canopy into two different kinds of vegetation. This is not done in this study. The characteristic values of Blue gramma grass are used for both vegetation types.

To run the model it is necessary to know the percentages of the maximum LAI for the six Julian weeks. These percentages can be determined from figure 4.2.1. The percentages are;

Julian week	percentage
136	40%
157	60%
164	70%
171	80%
178	90%
185	100%

6. The sensitivity of Vd_O3 for r_a and R_c

Investigating the sensitivity of the V_dO_3 can be useful to get an indication which quantities presented in chapter 3 need the most attention to improve the performance of the model. The sensitivity of the model is investigated for Julian week 157. Since the sensitivity increases with an increase in the percentage of maximum LAI, a percentage of 100% is used in the sensitivity analysis instead of the percentage of 60%. Most graphs that are presented in this chapter show only a selected amount of the data because of the improvement in resolution between the different curves.
In figure 6.1 the sensitivity of V_dO_3 for r_a is presented. Since c_v is the least certain factor in the calculation of r_a, the V_dO_3 is presented here as function of c_v. Figure 6.1 shows the V_dO_3 using a value of $c_v = 2$ and 2.64 for the whole stability range and the V_dO_3 using these two values dependent on the stability. The graph gives an indication about the error in V_dO3 introduced by using a value of $c_v = 2$, where a value of 2.64 should have been used and the opposite.

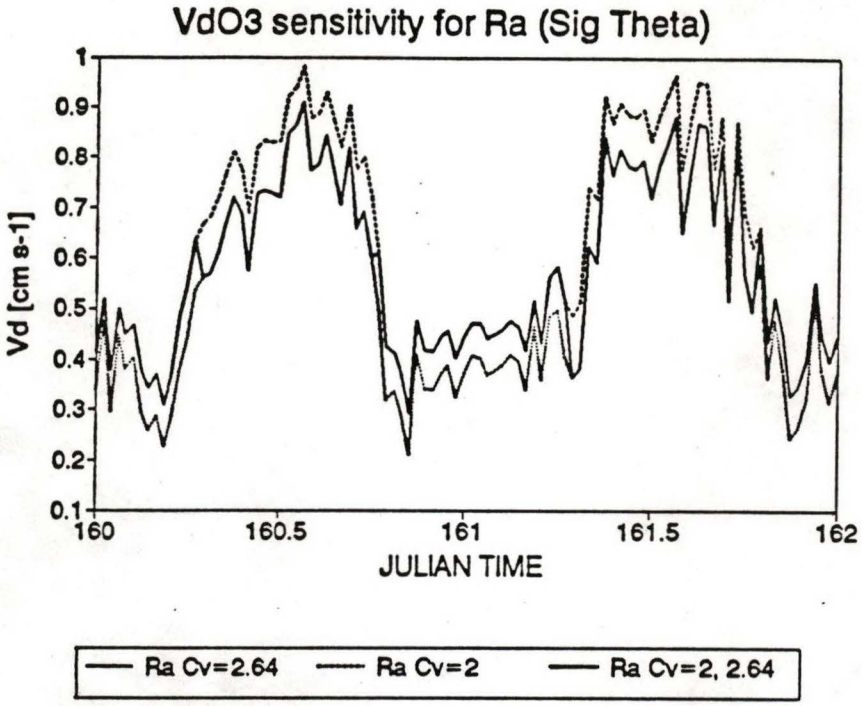

Figure 6.1.--The sensitivity of V_dO_3 for r_a (σ_θ).

As is shown in chapter 3, the R_c is determined by the integrated canopy resistance, R_{fol} and the $r_{sl}O_3$. R_{fol} is determined by r_{cut}, r_b and r_s ($r_{mes} = 0$ for ozone) and the LAI. r_{cut} has such a large value that the impact on the V_dO_3 of this term can be neglected. The minimal value of r_{cut} is 3000 s m^{-1}, in comparison with the parallel resistance r_s who has a typical value of about 100 s m^{-1} in the day-time. During the night, r_{cut} basically determines R_{fol} since r_s has a typical value of about 40.000 s m^{-1} during the night. However, R_{fol} is not relevant for the V_dO_3 determination during the night.
The sensitivity of V_dO_3 for r_b is shown in figure 6.2. V_dO_3 is presented for r_b calculated by equation 3.3.3 ($r_b$org) and $r_b$org plus and minus 10 s m^{-1}. It is obvious that the impact of r_b on V_dO_3 is minimal.

r_s is determined by r_{smin}, b', I_p and the correction factors f_t, f_w, f_v and f_s. In figure 6.3 the sensitivity of V_dO_3 for the minimal stomatal resistance r_{smin} is presented. The values used for r_{smin} are 50, 75, 100 and 125 s m^{-1}, are based on the r_{smin} of Bluegrass and on the values of r_{smin} that can be found for other kinds of vegetation present at the Pawnee site. r_{smin} of, for example, Agropyron Smithii, is about 125 s m^{-1} (Monson et al., 1986). Besides the Blue gramma grass the Stipa comata is a dominant vegetation in the immediate vicinity of the tower but unfortunately, there is not any information available concerning the r_{smin} of this vegetation. This is also one of the reasons that it is assumed that the whole canopy is formed by Bluegrass.
Figure 6.4 shows that the sensitivity of V_dO_3 for the light response coefficient b' can be neglected. Values of b' used for the sensitivity analysis are 35, 50 and 65 W m^{-2}.
Of the four correction factors, only the correction factor for temperature f_T is presented here because of its dependency on the
kind of vegetation. The other correction factors are not presented since f_w, f_w and f_s are determined in the model using specific quantities that are independent of the specific properties of the measurement location. f_t is determined by the characteristic minimal, optimum and maximum temperature (respectively T_e, T_o and T_h) of a specific kind of vegetation. The sensitivity of V_dO_3 for different values of T_e, T_o and T_h is shown in figure 6.5. Besides the model-derived V_dO_3 for the default values of T_e, T_o and T_h of respectively 5, 30 and 40 ^{0}C, V_dO_3 using values of respectively 5, 25 and 45 ^{0}C is shown. It is obvious that the impact of the temperature correction of the r_s on V_dO_3 can be neglected in this study.
In figure 6.6 the sensitivity of V_dO_3 for the LAI is presented. V_dO_3 is determined using a value of 0.5 (LAImax) and 0.35 (0.7*LAImax) for the LAI.

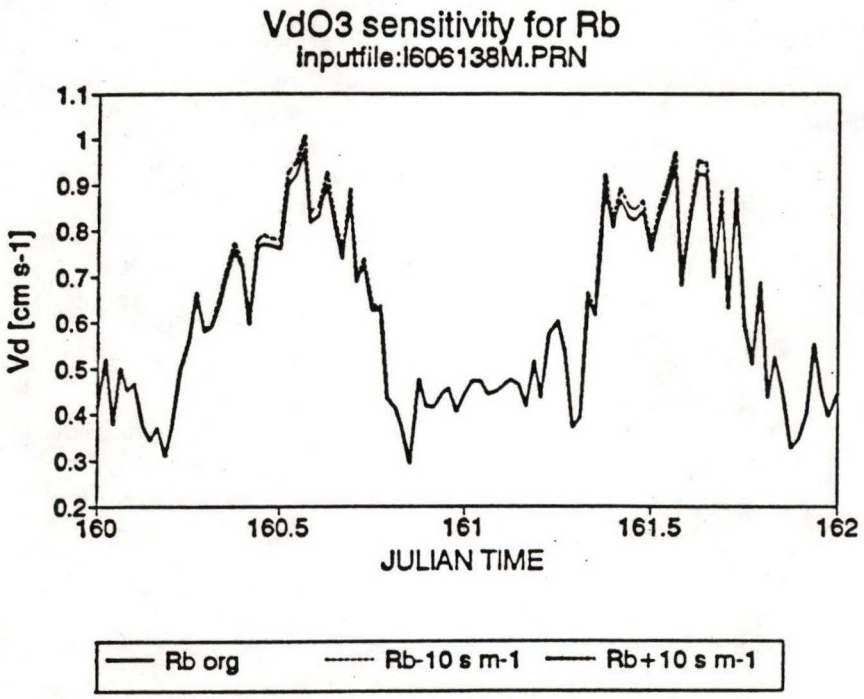

Figure 6.2: The sensitivity of V_dO_3 for r_b.

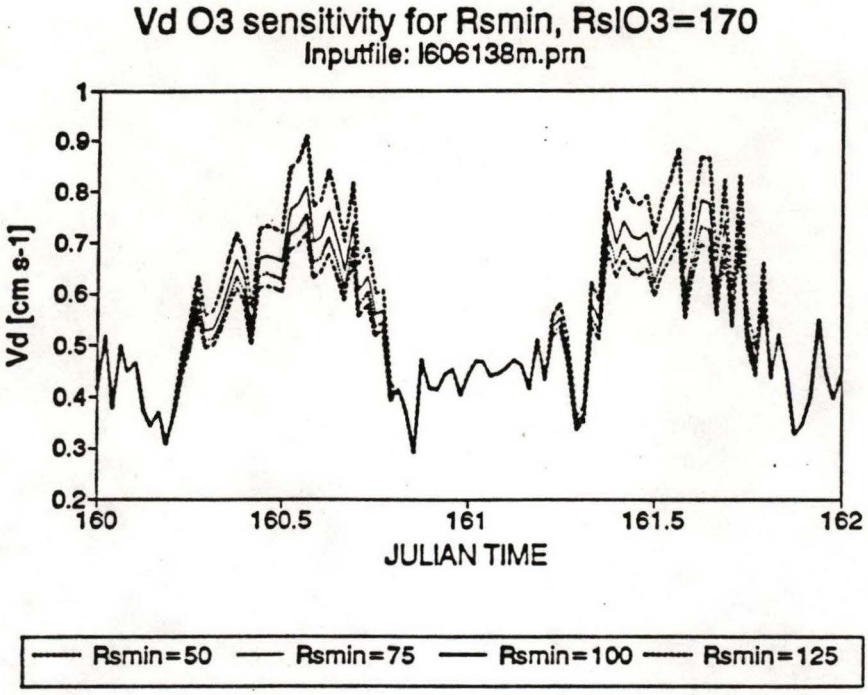

Figure 6.3: the sensitivity of V_dO_3 r_{smin}.

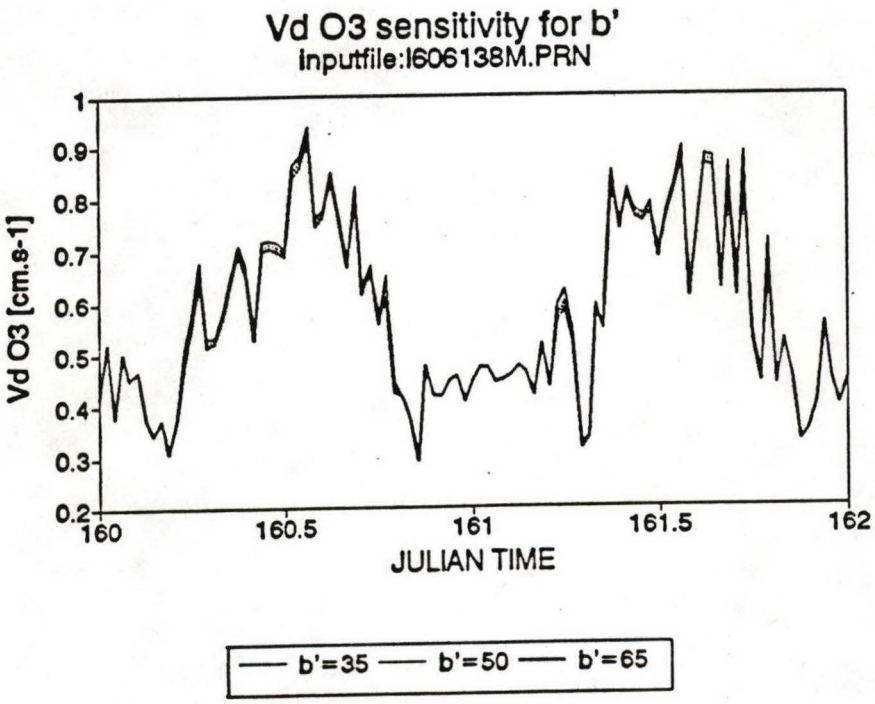

Figure 6.4: the sensitvity of V_dO_3 for b'.

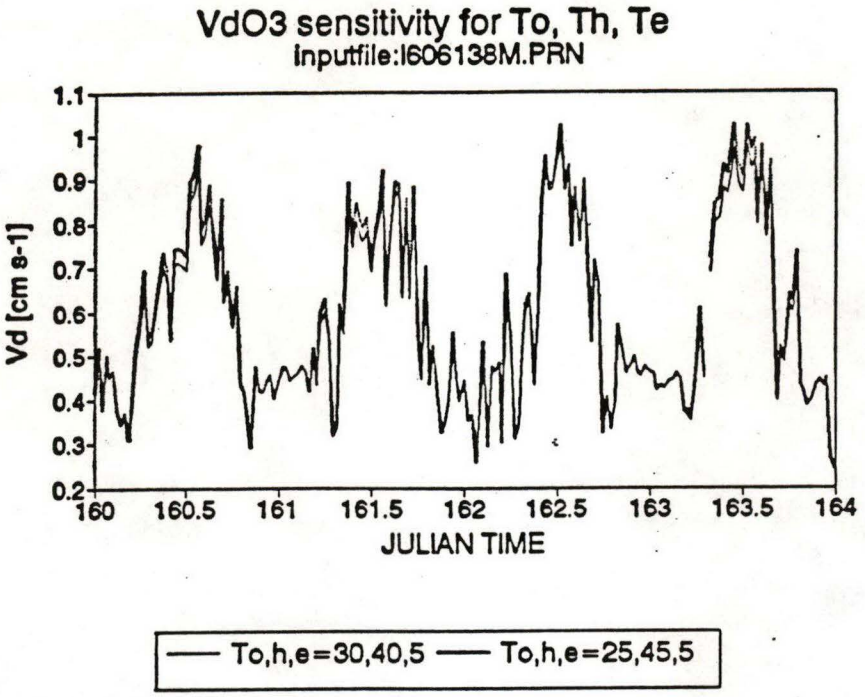

Figure 6.5: the sensitvity of V_dO_3 for T_e, T_h and T_e.

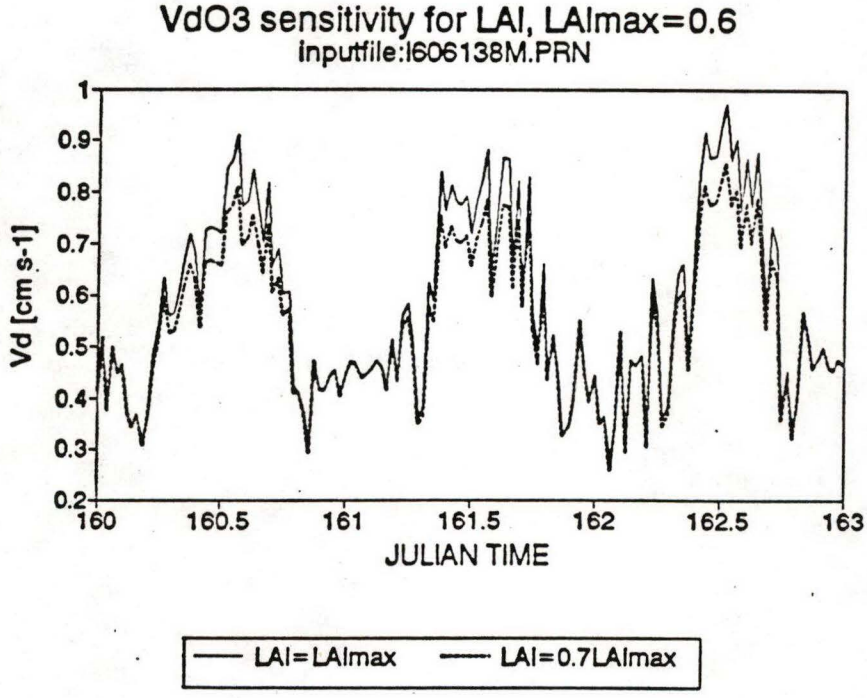

Figure 6.6: The sensitivity of V_dO_3 for LAI.

From figure 6.3 and 6.6, it is obvious that V_dO_3 is only sensitive to different r_{smin} and LAI values in the day-time. A change in r_{smin} and the LAI cause a change in the amplitude of the curve of V_dO_3. This is what can be expected since the stomatal resistance is basically determined by the photosynthetically active radiation (PAR). During the nights when the PAR is equal to zero, the stomatal resistance is extremely high. The stomatal resistance basically determines r_c and consequently R_{fol}. During the nights R_{fol} has a typical value of about 20.000 s m^{-1} and $r_{al}O_3$ of 170 s m^{-1}. This means, as can be seen in equation 3.3.8, that R_{fol} can be neglected in the determination of the total surface resistance R_c. Thus, V_dO_3 is basically determined by r_a and $r_{al}O_3$ during the nights. In figure 6.7 the dependency of V_dO_3 on $r_{al}O_3$ is presented. The different values of $r_{al}O_3$ are 170, 200, 400 and 600 s m^{-1}. These values are based on the value found by Massman of 170 s m^{-1} and on the value of $r_{al}O_3$ of a 1000 s m^{-1} used in the previous edition of the model. The value of $r_{al}O_3$ of 1000 s m^{-1} is not incorporated here in the sensitivity analysis because previous runs of the model indicated that this value is too high. Figure 6.5 shows that V_dO_3 is effected by $r_{al}O_3$ during the night as well as in the day-time. A decrease or an increase in $r_{al}O_3$ moves the whole curve to respectively a higher or lower level.

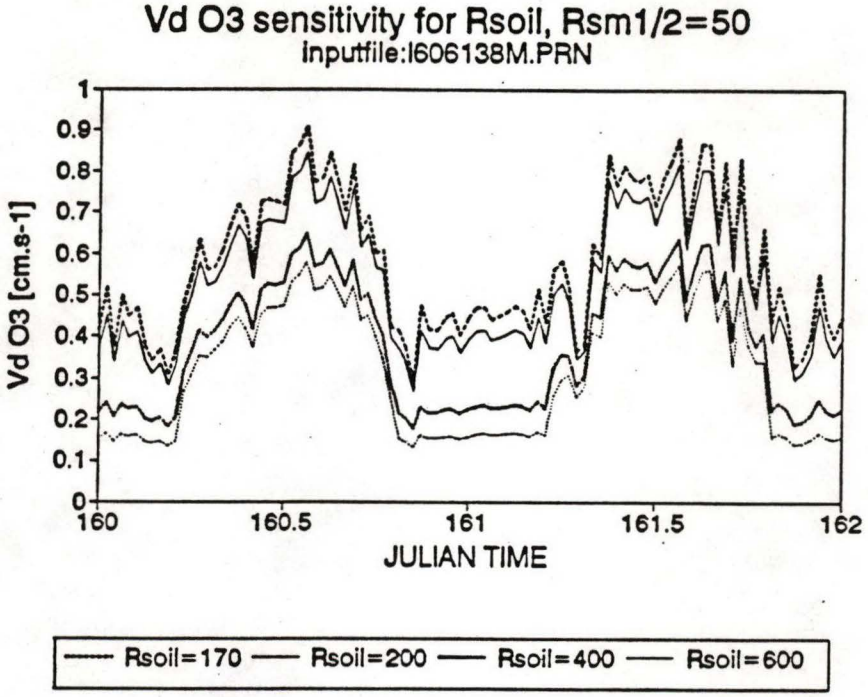

Figure 6.7: The sensitivity of V_dO_3 $r_{al}O_3$.

In table 6.1 the sensitivity of V_dO_3 for the quantities with the largest impact on V_dO_3 is presented in the form of the average and maximum $\Delta V_dO_3/\Delta X$ where X stands for the specific quantity. The figures concerning the sensitivity of V_dO_3 for r_{smin} and the LAI are those determined for the day-time.

Table 6.1: The sensitivity of V_dO_3 for r_a, r_{smin}, LAI and $r_{al}O_3$. In the third and fourth column the average and maximum $\Delta V_dO_3/\Delta X$ is shown. The used values of the resistance terms have the unit s cm^{-1}!

X	Change in input- values, ΔX	Average $\Delta V_dO_3/\Delta X$ [cm s^{-1}/unit X]	Max $\Delta V_dO_3/\Delta X$ [cm s^{-1}/unit X]
r_a	$r_a(c_v=2) - r_a(c_v=2.64)$ s cm^{-1}	-0.39	-1.11
r_{smin}	$50\text{-}75*10^{-2}$ $75\text{-}100*10^{-2}$ $100\text{-}125*10^{-2}$ s cm^{-1}	-0.24 -0.14 -0.092	-0.48
LAI	0.6 (LAImax) - 0.42 [ratio]	0.39	0.73
$r_{al}O_3$	$170\text{-}200*10^{-2}$ $200\text{-}400*10^{-2}$ $400\text{-}600*10^{-2}$ s cm^{-1}	-0.15 -0.07 -0.03	-0.27

7. Results

During the nights, R_{fol} can be ignored in the determination of the total surface resistance R_c since R_{fol} is extremely large compared with $r_{sl}O_3$. So, equation 3.1.1 can be rewritten to;

$$(7.1) \qquad V_dO_3 = \frac{1}{r_a + r_{sl}O_3}$$

This gives the opportunity to determine if the value for $r_{sl}O_3$ of 170 s m^{-1} can be accepted or if it must be adjusted. If it is assumed that $r_{sl}O_3$ does not show a diurnal cycle, $r_{sl}O_3$ can be estimated from the measured V_dO_3 and r_a during the nights. It can be expected that the uncertainty in the measured V_dO_3 and r_a will be larger during the night than during the day, because of the small values during the night of the quantities that determine these quantities. However, if all the data collected during the selected period are used, it must be possible to get an reasonable estimate of $r_{sl}O_3$. For this investigation, the corrected measured V_dO_3 data and r_a (z/L) are used.
The night data are selected from the data set using the selection criterion R_{fol} > 1000 s m^{-1}. The results of this $r_{sl}O_3$ determination are presented in table 7.1.

Table 7.1; $r_{sl}O_3$ estimated from the corrected measured V_dO_3 and r_a (z/L) during the night. The values presented here for $r_{sl}O_3$ are the 50-percentile values. In the third column the standard deviation is shown and N is the number of data.

Julian week	$r_{sl}O_3$ [s m^{-1}]	Std [s m^{-1}]	N
136	391	1075	95
157	237	379	102
164	367	5254	135
171	400	8597	105
178	436	79762	132
185	353	4021	118

The value of 170 s m^{-1} found by Massman, is significantly smaller compared with the values presented in table 7.1. The scatter in the values is large as is shown by the standard deviation of the estimated $r_{sl}O_3$. Criteria were used in order to delete the most extreme values but it did not a cause a significant difference in the 50-percentile values of $r_{sl}O_3$.
The model was run for every Julian week using a value of 170 s m^{-1} and also for the value of $r_{sl}O_3$ determined from the night data. Figure 7.1a,b,c,d,e, and f show the results of these simulations using the estimated $r_{sl}O_3$ for the six Julian weeks versus the corrected measured V_dO_3. Figure 7.1g shows V_dO_3 for $r_{sl}O_3$ = 170 s m^{-1} versus the corrected measured V_dO_3 for Julian week 171.
Figure 7.1a through f show an improvement of the performance of the model using the values of $r_{sl}O_3$ determined from the night data. Figure 7.1g shows that a value of 170 s m^{-1} for $r_{sl}O_3$ results in an overestimation of V_dO_3 of ± 0.25 cm s^{-1} for Julian week 171. This overestimation of V_dO_3 using $r_{sl}O_3$ = 170 s m^{-1}, can also be found for all the other Julian weeks.

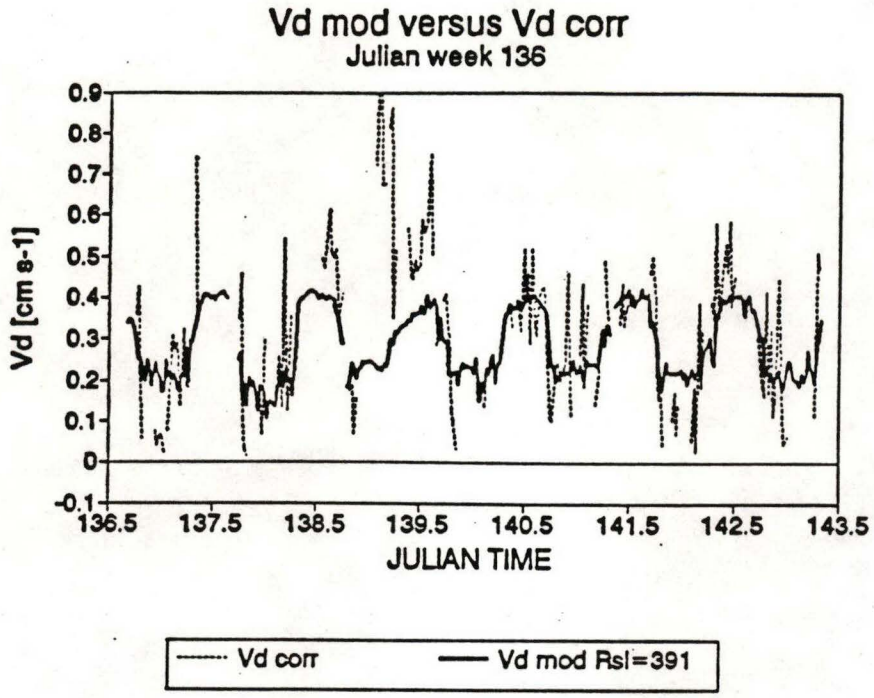

Fig. 7.1a.

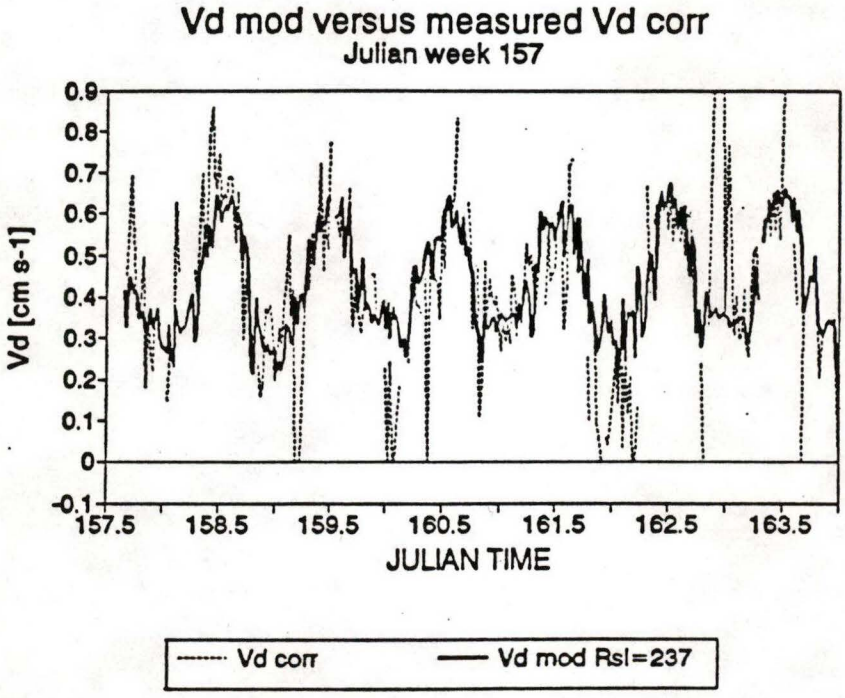

Fig. 7.1b.

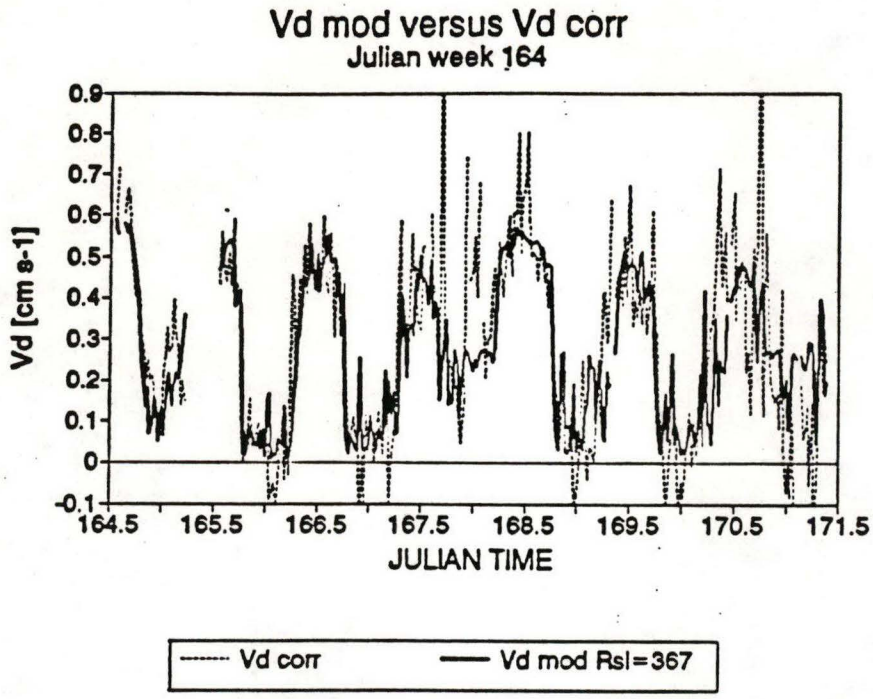

Fig. 7.1c.

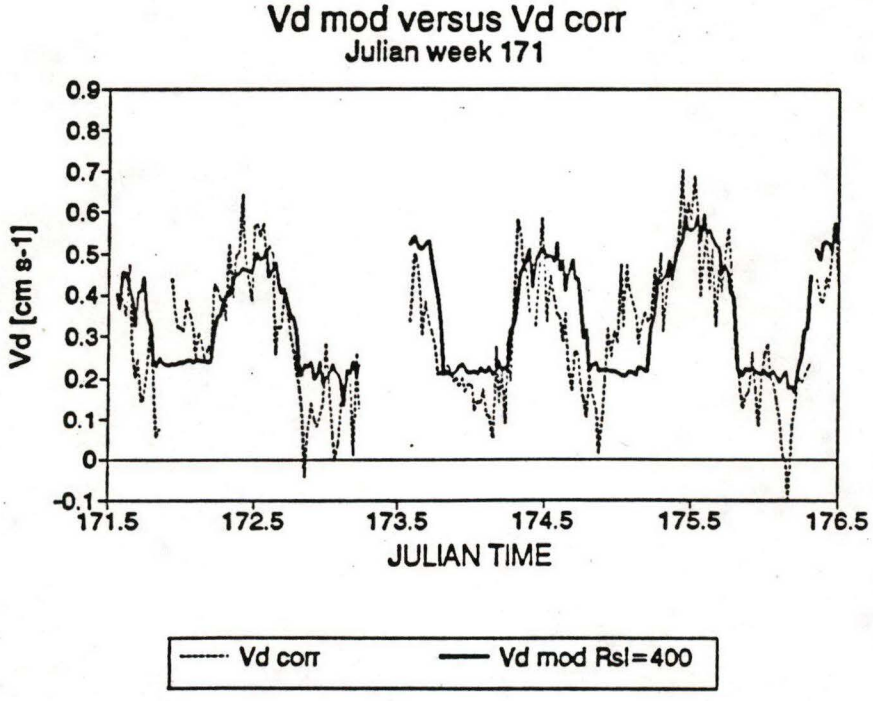

Fig 7.1.d.

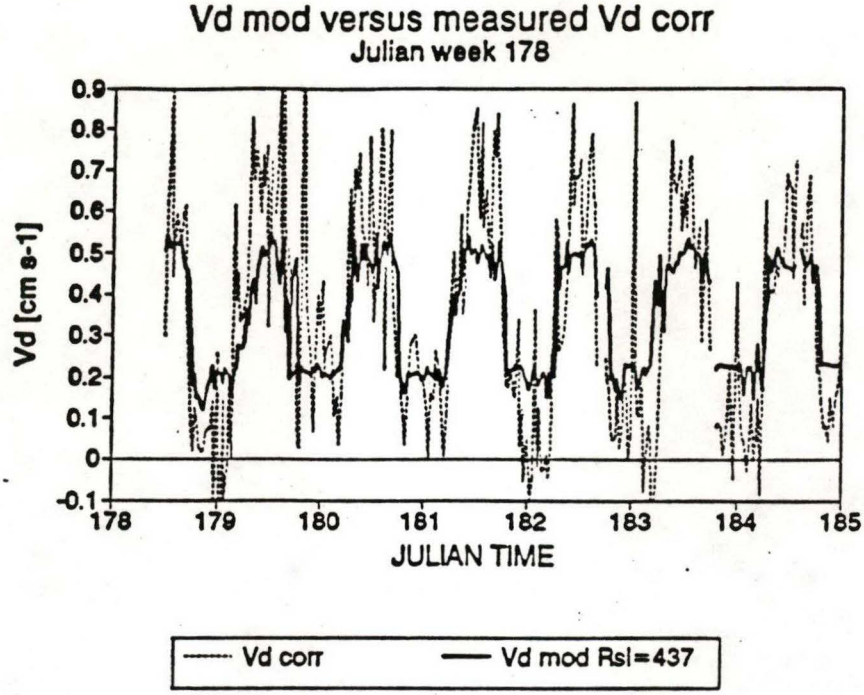

Fig. 7.1.e.

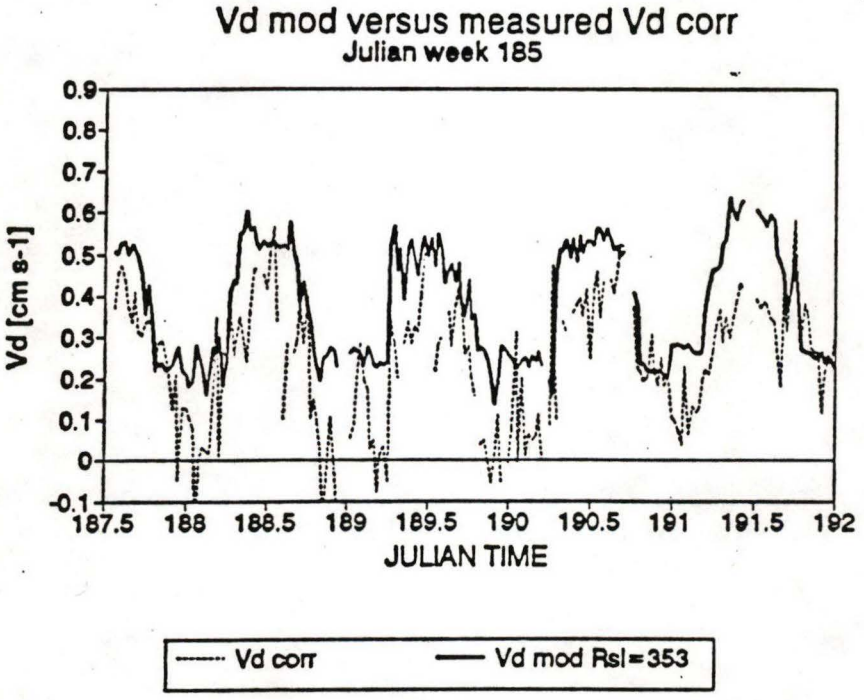

Fig 7.1.f.--Figure 7.1a,b,c,d,e and f.--The model-derived V_d and corrected measured V_d. V_d corr stands for the corrected measured V_d. The curve given by V_d mod Rsl=X, is the V_d calculated using a value for $r_{sl}O_3$ of X s m^{-1}.

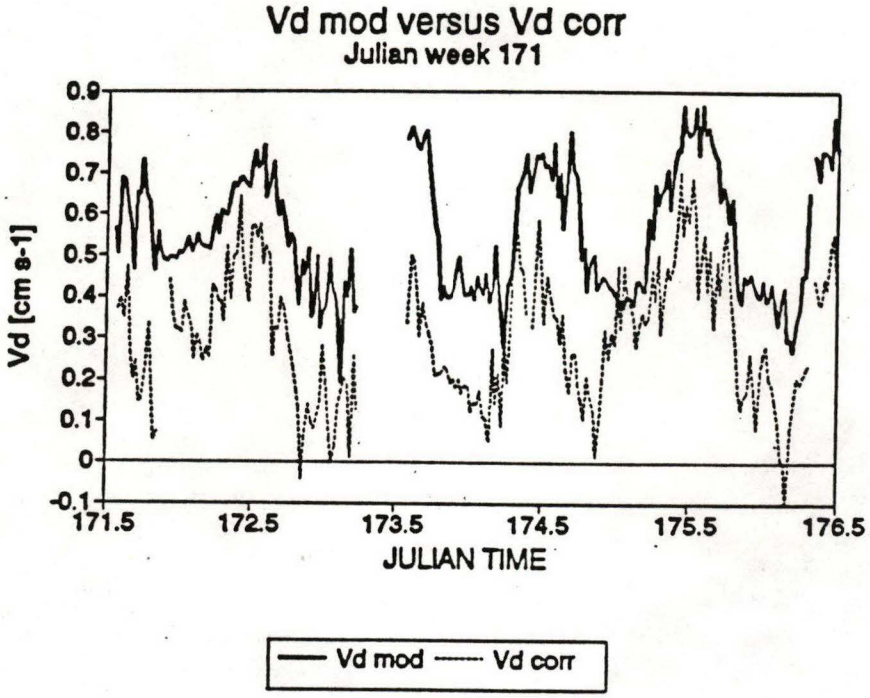

Figure 7.1g.--The model-derived V_dO_3 for $r_{sl}O_3 = 170$ s m^{-1} versus the corrected measured V_dO_3 for Julian week 171.

Table 7.2.--The average weekly V_dO_3 for the six Julian weeks. For definitions of the parameters see figure 7.1. The first line and second line of values are the average values for respectively in the day- and the night-time.

Julian week	V_d mod [cm s^{-1}]	V_d corr [cm s^{-1}]	V_d mod R_{sl} [cm s^{-1}]	N
136	0.60	0.43	0.37	88
	0.40	0.24	0.22	99
157	0.62	0.53	0.58	116
	0.41	0.36	0.38	101
164	0.55	0.42	0.38	164
	0.23	0.12	0.13	139
171	0.68	0.40	0.40	125
	0.43	0.20	0.22	105
178	0.66	0.48	0.44	191
	0.44	0.14	0.20	136
185	0.66	0.33	0.48	131
	0.43	0.14	0.24	113

For all the six Julian weeks, V_dO_3 is integrated over the whole week in order to show the performance of the model concerning the prediction of the total amount of deposited ozone over a longer period. Normally, the ozone flux is used for this integration in order to determine the absolute values of deposited ozone (ppb m^{-2}). However, in this study the relative values of deposited ozone are more relevant. In that case it is not necessary to recalculate the integrated V_dO_3 to the integrated O_3-flux by multiplying V_dO_3 with the O_3-concentration. Table 7.2 shows the integrated V_dO_3 for all the six Julian weeks. The integrated V_dO_3 is divided by the amount of data N in order to correct for differences in N between the six Julian weeks. So, actually the average weekly V_dO_3 is presented. Except of Julian week 185, the differences between the average weekly corrected measured V_dO_3 and model-derived V_dO_3 for the estimated $r_{sl}O_3$, are not larger than 0.06 cm s^{-1} as well in day- as the night-time.

A certain caution has to be incorporated in any conclusion concerning the improvement of the performance of the model in the day-time because of the impact of R_{fol} on the V_dO_3 in day-time. The R_{fol} is calculated in the model, based on the assumption that the whole canopy is formed by Bluegrass. This can cause an overestimation of the V_dO_3 because of the small r_{smin} value for Bluegrass compared with r_{smin} of the other kinds of vegetation at the site. Massman (1992) found a typical value for r_{ctot} of about 400 s m^{-1} for the Pawnee site in the day-time for Julian day 166 in 1989. Using a value of 50 s m^{-1} for r_{smin} in the model results in a r_{ctot} of about 100 s m^{-1} for the same day. A value of 125 s m^{-1} for r_{smin} (Agropyron Smithii) or even larger, results in a average value of r_{ctot} that is in better agreement with the value found by Massman. Using r_{smin} = 125 s m^{-1} instead of 50 s m^{-1} will cause an average decrease in V_dO_3 of ± 0.12 cm s^{-1} (see table 6.1). Figure 7.2a shows V_dO_3 determined using r_{smin} = 125 s m^{-1} for Julian day 166 through 169. The amplitude of the diurnal cycle of V_dO_3, which is basically determined by r_{smin}, is too small. The same underestimation of V_dO_3 using r_{smin} = 125 s m^{-1}, was also found for the other Julian weeks. There will also be a contribution into the uncertainty in r_{ctot} and so in V_dO_3, caused by the uncertainty in the LAI. Assuming that the error in the LAI will be about 0.1, this will cause an error in V_dO_3 of ± 0.04 cm s^{-1}.

The results presented so far, are all based on the assumption that $r_{sl}O_3$ does not show a diurnal cycle. If $r_{sl}O_3$ shows a diurnal cycle, characterized by an decrease in the day-time compared with the night-time, then this parameter will also have an impact on the amplitude of V_dO_3. It is possible to estimate the magnitude of the decrease in $r_{sl}O_3$ in the day-time. Assuming that r_{smin} = 125 s m^{-1}, resulting in a r_{ctot} in better agreement with the value found by Massman, it can be estimated from figure 7.2a and table 6.1 that $r_{sl}O_3$ must decrease to a value of about 170 s m^{-1} in the day-time for Julian week 164. This decrease in $r_{sl}O_3$ is needed to compensate for the decrease in the amplitude of V_dO_3 caused by the increase in r_{smin}. Figure 7.3 shows the model-derived V_dO_3 for r_{smin} = 50 s m^{-1} and a constant value of $r_{sl}O_3$ = 367 s m^{-1} for the whole day (V_d mod Rsl=437) and V_dO_3 for r_{smin} = 125 s m^{-1}, $r_{sl}O_3$ = 170 s m^{-1} when the global radiation R_G > 10 W m^{-2} and $r_{sl}O_3$ = 367 s m^{-1} for R_G < 10 W m^{-2} (V_d mod Rsl=170). There is only a significant difference between the two curves concerning the absolute level in V_dO_3 and not concerning the fluctuation. Thus, the only error that will be introduced in V_dO_3 by ignoring the diurnal cycle, is an error in the absolute level of V_dO_3.

Soil temperature and soil moisture are two parameters that will play a role in determining the diurnal cycle of $r_{sl}O_3$. It can be expected that $r_{sl}O_3$ will decrease in the day-time caused by an increase in the soil temperature. An increase of soil moisture will also cause an decrease of $r_{sl}O_3$ but this effect is probably more relevant on a longer time scale. Figure 7.4a and b show the estimated $r_{sl}O_3$ versus the average weekly soil temperature and the precipitation. Except of the significant smaller $r_{sl}O_3$ after the precipitation in the first week of June, there is not any distinct correlation visible between $r_{sl}O_3$ and the precipitation or soil temperature.

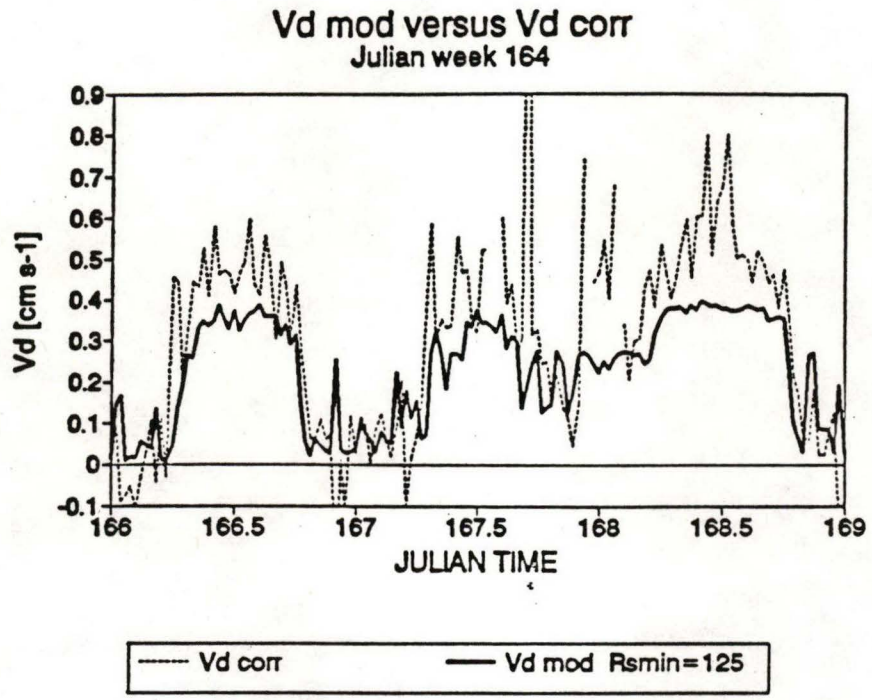

Figure 7.2.--V_dO_3 determined using a value of 125 s m^{-1} for r_{smin} versus the corrected measured V_dO_3 for Julian day 166 through 169.

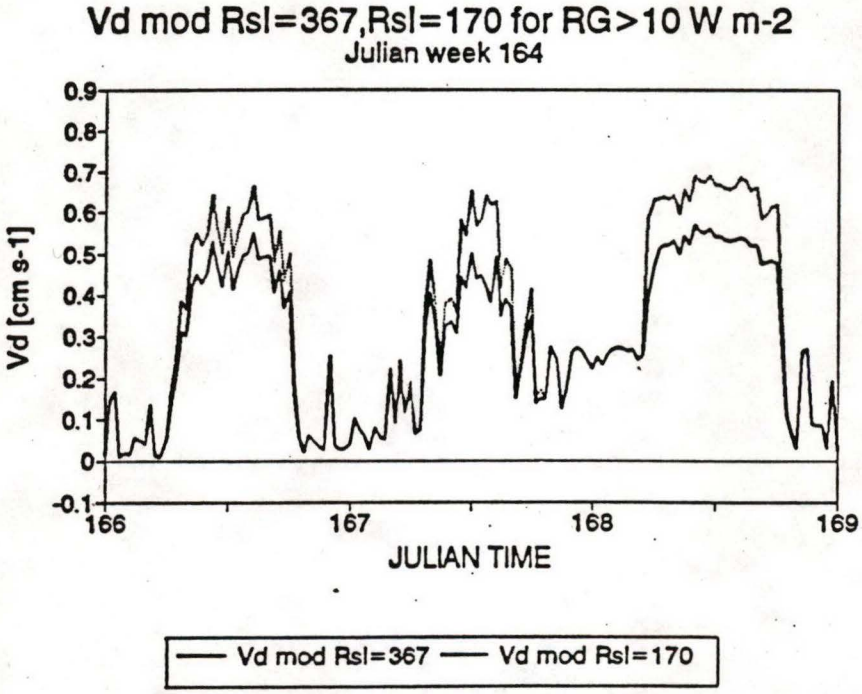

Figure 7.3a.--The model-derived V_dO_3 for Julian day 166 through 169. V_d mod Rsl=367 stands for the model-derived V_dO_3 for r_{smin} = 50 s m^{-1} and $r_{sl}O_3$ = 367 s m^{-1} for the whole day. V_d mod Rsl=170 stands for V_dO_3 for r_{smin} = 125 s m^{-1}, $r_{sl}O_3$ = 367 s m^{-1} for R_G < 10 W m^{-2} and $r_{sl}O_3$ = 170 s m^{-2} for R_G > 10 W m^{-2}.

Concerning the night data, the agreement between the model-derived and corrected measured V_dO_3 improves for all the six Julian weeks using the estimated values for $r_{al}O_3$ instead of 170 s m^{-1}. However, there is only a better agreement concerning the absolute values of V_dO_3. The figures show that the agreement in the fluctuations decreases. The contribution of $r_a(\sigma_\phi)$, the quantity that is basically responsible for the fluctuations in V_dO_3, into the total resistance decreases because of the increase of $r_{al}O_3$. The figures for the Julian weeks 136, 171,178 and 185 show this shortcoming of the model. For Julian week 157, $r_{al}O_3$ is so small that $r_a(\sigma_\phi)$ can play a significant role in determining V_dO_3, at least in the fluctuations in V_dO_3. The reasonable good agreement between the measured and the model-derived V_dO_3 for Julian week 164 can basically be attributed to an average larger $r_a(\sigma_\phi)$, especially during the night. Figure 7.5a and b show the residual r_a, $r_a(\sigma_\phi) - r_a(z/L)$, and σ_ϕ for Julian week 164 and 178. For Julian week 164, during the night ra (σ_ϕ) is in general overestimated compared to r_a (z/L). On the contrary, for Julian week 178, $r_a(\sigma_\phi)$ is in general underestimated during the night. The cause of this over- and underestimation for respectively week 168 and 178 can basically be contributed to σ_ϕ. In Julian week 164, the average minimal value of σ_ϕ was about 0.025 during the night. For Julian week 178, this average minimal value was about 0.05. For example, for an average windspeed of about 2 m s^{-1} this would cause a difference in $r_a(\sigma_\phi)$ of 2400 s m^{-1}. Plots of σ_ϕ for the other Julian weeks indicate that the small value of σ_ϕ for Julian week 164 is more exception than rule. The graph of the residual r_a and σ_ϕ for Julian week 178 is a representative graph for the other Julian weeks except of 164.

Finally, figure 7.5a shows the model-derived V_dO_3 using respectively the input-data of the RMFRES measured at 3 m and 8 m height for Julian time 157.5 through 161.5. Figure 7.5b shows the difference in V_dO_3 caused by using the NOAA-data measured at 10 m height instead of the RMFRES-data measured at 8 m height. There is not any significant difference in the day-time between the V_dO_3 determined using the input-data measured at 3 m and 8 m height. The differences between the two curves in the night-time are caused by small differences in σ_ϕ. As explained earlier in this chapter, a small change in σ_ϕ under stable conditions (generally a small σ_ϕ) can cause a large change in $r_a(\sigma_\phi)$. Using the 10 m data instead of 8 m data causes, as expected, a small increase in V_dO_3 as well in the day-time as during the night.

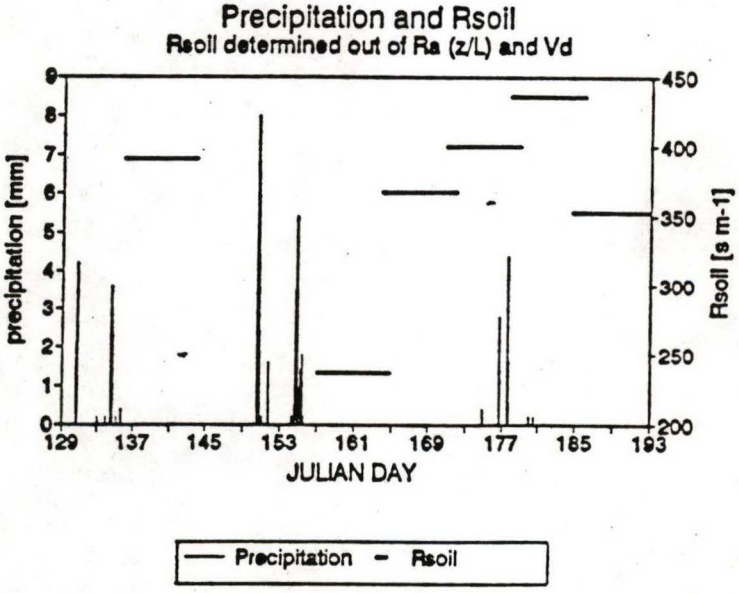

Figure 7.4a.--The estimated $r_{al}O_3$ versus the precipitation for Julian day 129 through 193.

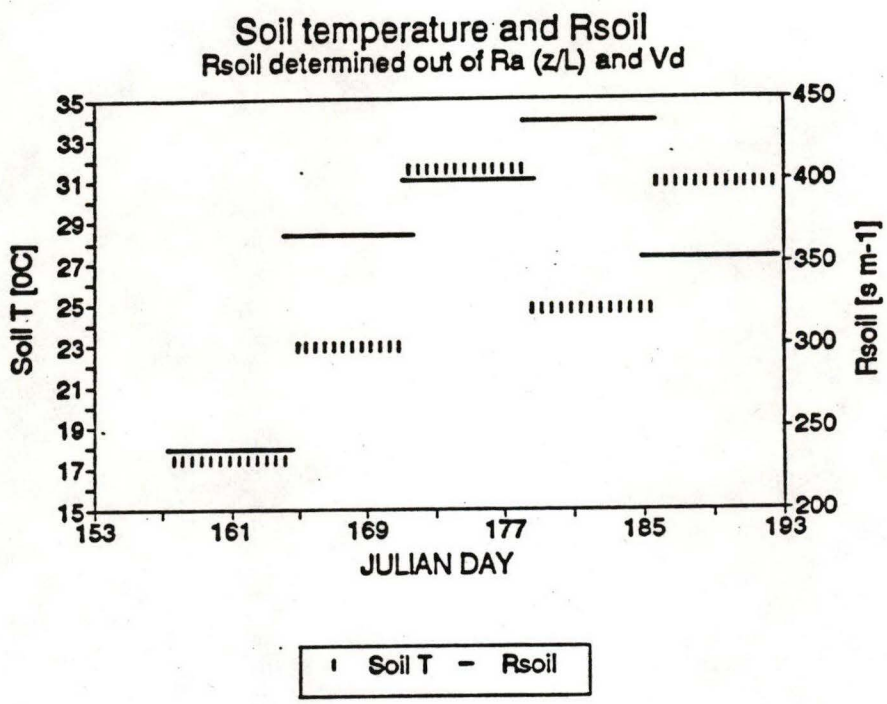

Figure 7.4b.--The estimated $r_{a1}O_3$ versus the average weekly soil temperature.

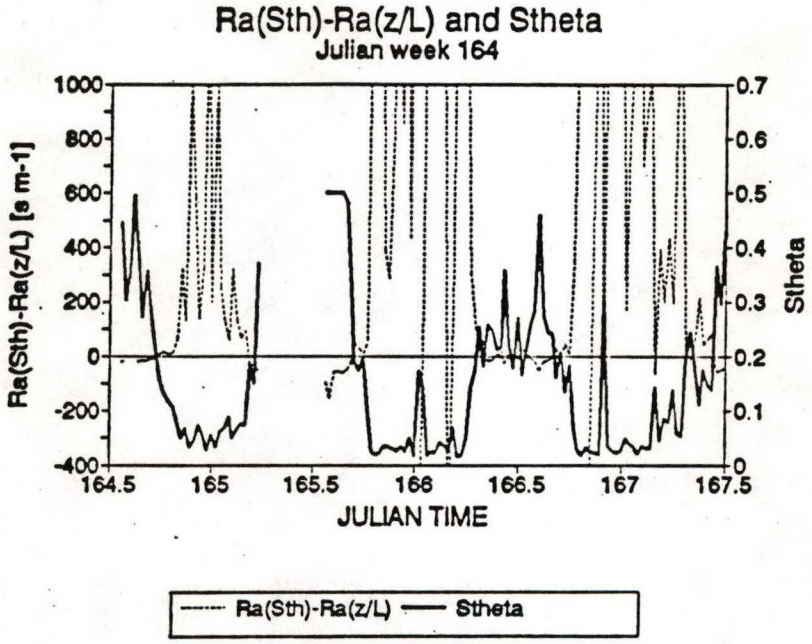

Figure 7.5a.--The residual r_a, $r_a(\sigma_\theta)$- $r_a(z/L)$ and σ_θ for Julian time 164.5 through 167.5.

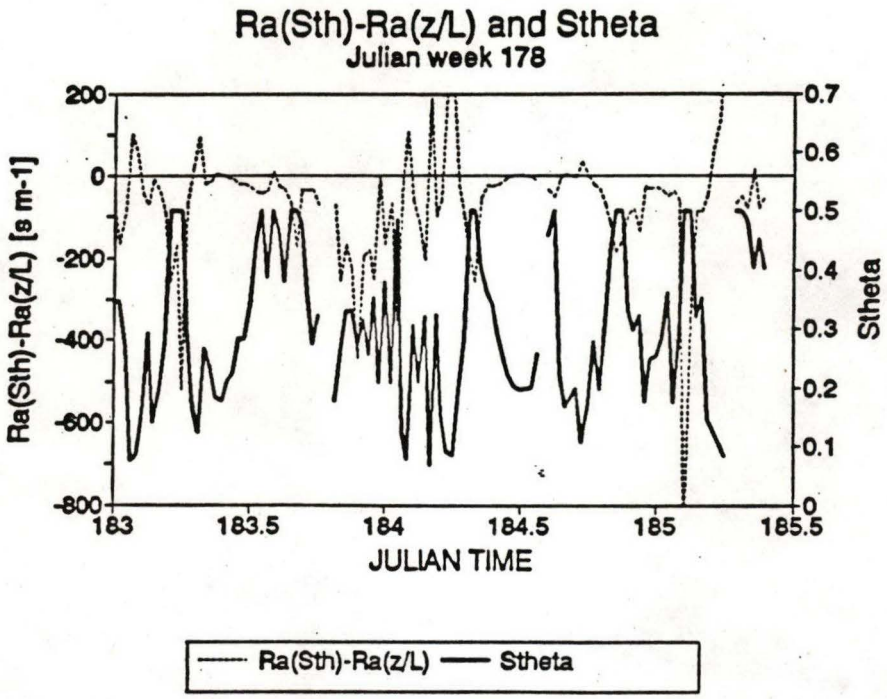

Figure 7.5b.--The residual r_a, $r_a(\sigma_\theta)$-r_a (z/L) and σ_θ for Julian time 183.0 through 185.5.

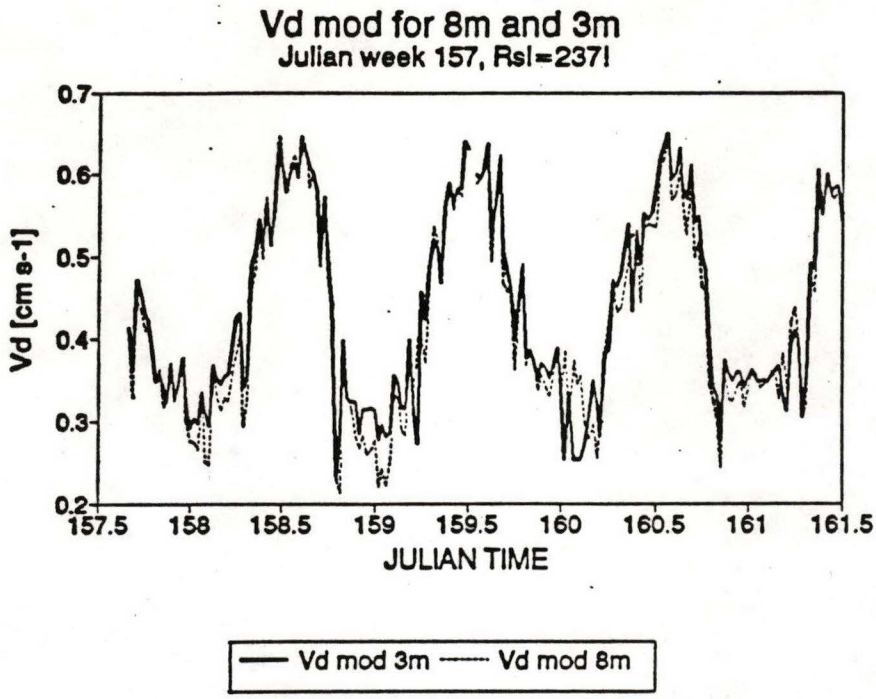

Figure 7.5a.--The model-derived V_dO_3 using the input-data of the RMFRES measured at 3 m and 8 m height.

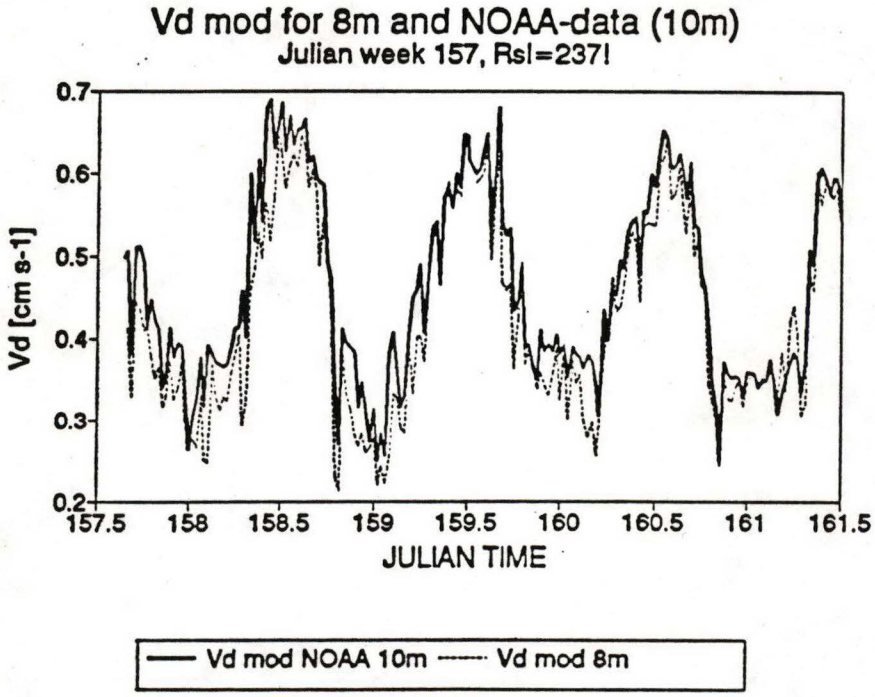

Figure 7.5b.--The model-derived V_dO_3 using the input-data of the RMFRES measured at 8 m height and NOAA, measured at 10 m height.

8. Conclusion

The sigma theta method does not estimate r_a with large precision. The determination of the specific c_v values for the Pawnee-site and an attempt to improve the distinction between the different stability classes out of the small selection of input-data, did not cause an improvement in r_a. There is disagreement between the measured and model-derived V_dO_3 concerning the fluctuations. Especially in the night-time, the sigma theta method underestimates r_a. An improvement is needed in the sigma theta method under stable conditions. During the investigation to determine the specific c_v values, it seemed that an increase of the c_v value with an increase in stability under stable conditions must result in a better estimate of r_a in the night-time. However, this is not relevant for the model since it is not possible to determine the stability with such an accuracy out of the small selection of input data.
It seems that the performance of the model improves using the method to determine $r_{sl}O_3$ out of the measured V_dO_3 and r_a (z/L) for the night data. However, the restricted selection of data normally used to run the model will only make it possible to determine r_a (σ_θ). Based on the underestimation of r_a (σ_θ) compared with r_a (z/L) in the night-time, the method to determine $r_{sl}O_3$ out of the night data will result in a overestimation of $r_{sl}O_3$ as long as the determination of r_a (σ_θ) does not improve under stable conditions.
The assumption that $r_{sl}O_3$ does not have a diurnal cycle is made in this study because there is not any information available at this moment concerning the magnitude of the amplitude of this diurnal cycle. Ignoring the diurnal cycle does not cause a worse performance of the model concerning the fluctuations in V_dO_3. Concerning the absolute level of V_dO_3, ignoring the diurnal cycle and the estimated $r_{sl}O_3$ out of the night data, probably causes an underestimation of V_dO_3 in the day-time. However, there is compensated for this underestimation by r_{ctot} which is probably too small. However based on all the information available concerning the vegetation at the Pawnee-site, choosing $r_{smin} = 50$ s m^{-1} and assuming that the whole canopy is formed by Bluegrass, seems at this moment the most reasonable solution of defining the vegetation at the Pawnee-site for the model. The first step of a better approach would be improvement of the determination of r_{ctot}, in order to make it possible to investigate the contribution of $r_{sl}O_3$ into the amplitude of V_dO_3. As long as there will be the uncertainty in as well the contribution of the vegetation as the soil in the deposition of ozone, not any conclusion can be made concerning the decrease in $r_{sl}O_3$ in the day-time.

Using $r_{smin} = 50$ s m^{-1} and the estimated $r_{sl}O_3$ out of the night data results in a reasonable agreement between the model-derived and measured V_dO_3, especially for Julian week 157 and 164. The worse agreement, especially concerning the fluctuations, for the other four Julian weeks is caused by a combination of small r_a (σ_θ) values and a large $r_{sl}O_3$. For Julian week 185, $r_{sl}O_3$ is probably underestimated, resulting in an overestimation of V_dO_3 over the whole week besides the small agreement concerning the fluctuations. The total amount of deposited ozone during a whole week is estimated by the model with reasonable accuracy. Except of Julian week 185, the differences between the average weekly corrected measured V_dO_3 and model-derived V_dO_3 are not larger than 0.06 cm s^{-1} as well in day- as the night-time.

Acknowledgement

I would like to thank the RMFRES, especially R. Musselman and Karl Zeller for giving me the opportunity to get my internship at the RMFRES. I also would like to thank W.J. Massman for sharing his ideas and knowledge and the co-editors of this paper G. Woolderidge and Lynn Utzman. They have given me some good ideas concerning my English wordchoice. Finally, I would like to thank Claudia, my roommate, for not understanding the Dutch language so that I could swear at the computer without offending any person.

Literature

Businger J.A., 1986, Evaluation of the accuracy with which dry deposition can be measured with current micrometeorological techniques, Journal of Climate and applied Meteorology, vol. 25, pag 1100-1123.

Cionco R.M., 1972, A wind-profile index for canopy flow, Boundary Layer Meteorology 3, pag 255-263.

Erisman J., Duyzer J., 1991, A micrometeorological investigation of surface exchange parameters over heathland, Boundary Layer Meteorology 57, pag 115-128.

Hazlett D.L., 1992, Leaf area development of four mplant communities in the Colorado steppe, The American Midland Naturalist 127;276-289.

Hicks B.B., Baldocchi D.D., Meyers T.P., Hosker JR. R.P., 1987a, A preliminary multiple resistance routine for deriving dry deposition velocities from measured quantities.

Hicks B.B., Matt D.R., 1987b, Combining Biology, chemistry and meteorology in modeling and measuring dry deposition, Journal of Atmospheric Chemistry 6, pag 117-131.

Massman W.J., 1992, Partitioning ozone fluxes to sparse grass and soil and the inferred resistances to dry deposition, Rocky Mountain Forest Range and Experiment Station, Fort Collins, Colorado.

Meyers T.P., 1987, The sensitivity of modeled SO_2 fluxes and profiles to stomatal and boundary layer resistances, Water,Air and Soil pollution 35 (1987), pag 261-278.

Zeller K.F. et.al., 1989, Initial results from the Pawnee eddy correlation system for dry acid deposition research, RM-282, Rocky Mountain Forest Range and Experiment Station, Fort Collins, Colorado.

Zeller K.F., 1990, Eddy diffusivities for sensible heat, ozone and momentum from eddy correlation and gradient measurements, dissertation paper, Civil Engineering Department, Colorado State University, Fort Collins, CO.

Appendix A

In this appendix, two inputfiles with their specific information are presented. Not presented here are the inputfiles LANG.SPH and PADPROF1,2,3.DAT which both contain information concerning the structure of the canopy like the distribution of the LAI over the different layers of the canopy.

Inputfile:PLANT.DAT

'SPRUCE',225,40,9,35,-5,2,23
'POND/LODGP PINE',500,40,25,5,40,3,23
'LOBLOLLY PINE',200,55,25,40,5,3,23
'WHITE OAK',100,50,25,45,5,2,23
'CHEST/N.RED OAK',100,40,25,45,5,2,23
'MAPLE',100,50,25,45,5,2,20
'WHITE BIRCH',300,40,25,40,5,2,23
'BEECH',100,50,25,40,5,2,20
'MAIZE',250,65,25,45,5,1,2.5
'WHEAT',100,25,25,40,5,1,1
'SOYBEAN',100,50,25,45,10,1,1
'GRASS',125,50,25,45,5,1,0.5
'BLUE GRASS',125[1],50[2],30[3],40[4],5[5],1[6],0.5[7]

See Blue grass;

1) = r_{smin}
2) = b'
3) = optimum temperature
4) = maximum temperature
5) = minimal temperature
6) = index for profile of the canopy
7) = canopy height

Inputfile:STATION.DAT

1,'OAK RIDGE',4,70,3.5,0.01,3,30,1.5,1.5,35.96,84.28,5,0
2,'WEST POINT',6,60,3.0,0.01,4,30,2.0,0,41.35,74.05,5,0
3,'WHITEFACE MOUNTAIN',7,70,4.2,0.01,6,30,1.8,0.01,44.39,73.86,5,0
4,'PENN STATE',9,50,4.0,0.01,4,50,5.0,0.01,40.72,77.92,5,1
5,'ARGONNE NAT LAB',4,50,4.0,0.01,11,50,2.0,0.01,41.7,87.98,6,1
6,'BONDVILLE IL',9,50,4.0,0.01,11,50,4.0,0.01,40.05,88.37,6,1
7,'PANOLA STATE PARK',3,50,4.0,4.0,4,50,2.5,0.01,33.63,84.18,5,1
8,'BORDEN, ONTARIO, CANADA',0,0,0,0,0,0,0,0,0,0,5,0
9,'SEQUOIA NAT PARK',11,60,2.8,0.01,2,35,1.8,1.8,36.58,118.75,8,0
10[1],'PAWNEE GRASSL[2]',13[3],70[4],0.33[5],0.01[6],13[7],30[8],0.17[9],0.01[10],40.82[11],104.77[12],7[13],0[14]
11,'OAK RIDGE TOWER',4,70,3.5,0.01,3,30,1.5,1.5,35.96,84.28,5,0
12,'SHENANDOAH NATPARK',5,70,3.5,0.01,6,30,1.5,0.01,38.63,78.38,5,0
13,'HOWLAND NAT FOREST',1,95,5.5,5.5,7,5,.3,0.01,45.17,68.77,5,0
14,'HUNTINGTON FOREST',8,72,4.7,0.01,6,28,1.8,0.01,44.98,74.25,5,0

See the Pawnee grasslands;

1) = station index
2) = station location

3) = first vegetation type
4) = percentage of LAImax for the first vegetation type
5) = absolute value of LAI for the first vegetation type
6) = winter LAI for the first vegetation type
7) = second vegetation type
8) = percentage of LAImax for the second vegetation type
9) = absolute value of LAI for the second vegetation type
10) = winter LAI for the first vegetation type
11) = latitude of station location
12) = longitude of station location
13) = zone (used in calculation of zenith angle
14) = index for averaging scheme (0 = canopy mix, 1 = area weighing)

Appendix B

FLOW SCHEDULE OF PROGRAM: DRYDEP2.FOR.

initialization of variables and parameters

↓

reading of inputfile (vegetation data)

↓

opening of input- (meteo) and outputfile

↓

calculations mainly concerning the LAI

↓

129 reading of inputfile (meteo) end=97

↓

IF (data >= 9999.99) THEN

← GO TO 85

ELSE

recalculations (STHETA)

↓

CALL SOILRESS → see SUBROUTINE SOILRESS

↓

computation RA

↓

computation of U_*

↓

set RCUT for dry or wet surface

CALL WETRESS → see SUBROUTINE WETRESS

↓

computation of ZEN (zenith angle) and RC

CALL ZENGEN → see SUBROUTINE ZENGEN

↓

IF (RG (global radiation) < 10 ($W.m^{-2}$) OR

ZEN > 2PI/4 (=90^0) THEN

IDAY=0

RVD (diffuse visible radiation) = 0.01

RBVD (visible beam radiation) = 0.01

FSL (fraction of sunlit leaves) = 0

ELSE IDAY=1

CALL WSTRESS → see SUBROUTINE WSTRESS

ENDIF

↓

```
computation of canopy resistance using two averaging
schemes (canopy mix or area weighing)

IF (AVER = 0) THEN (canopy mix)
        CALL WNDPROF  →          see SUBROUTINE WNDPROF
        IF (IDAY > 0) THEN
                CALL CANRAD2 → see SUBROUTINE CANRAD2
                (calling of TSTRESS, CANRES for species 1 and 2)
                (1,2) CALL TSTRESS  →  see SUBROUTINE TSTRESS
                CALL CANRES  →  see SUBROUTINE CANRES

                        ↓
        DO FOR L=1 TO NSCP (number of chemical species)
                VD(L) = 100/(RA + 1/(1/RC(L,1) +1/RC(L,2)+
                    1/RSOIL(L)))

ELSE (area weighing)
        DO FOR L=1,2
                CALL WNDPROF
                IF (IDAY > 0) THEN
                        CALL CANRAD2
                        CALL TSTRESS
                        CALL CANRES

                        ↓
        DO  FOR L=1 TO NSCP
                RC(L,1) = 1/(1/RC(L,1) + 1/RSOIL(L))
                RC(L,2) = 1/(1/RC(L,2) + 1/RSOIL(L))

        VD(L) = (PRCTN(1)/(RA + RC(L,2)) + PRCNT(2)/
                  (RA + RC(L,2))
        (PRCNT is percentage of max. leaf area index)
END IF

                        ↓
computation of particle deposition velocity
VD(4) = 100/(1/(.002*(U*)) + RA)

IF (STHETA > .175) AND (RG > 250) THEN
        VD(4) = 100/(1/(.03*USTAR + RA)
END IF

                        ↓
85      writing of calculated values to outputfile:
        VD's for all chemical species and particles, RA, RB,
        and RC and the inputdata.

                        ↓
        GO TO 129

97      CLOSE INPUTFILE

        END
```

SUBROUTINE SOILRESS

input: SOIL, SNOW, TA
output: SOIL

initialization of SOIL(1,2,3)

IF (SNOW > 0) THEN
    SOIL(1,2,3) = new value
    IF (TA < -2) THEN
        SOIL(1,2,3) = new value
        (TA = absolute dry air temperature in ^{0}C)
END IF

END

SUBROUTINE WETRESS

input: RCUT, CWET, RAIN
output: RCUT, (IWET=help variable)

detection of surface wetness
IF (IWET = 0) AND (CWET > .5) THEN
    IWET = 1
(CWET = canopy wetness (0 - 1))

↓

wetness caused by rain ?
IF (RAIN > 0) IWET = 2

↓

IF (CWET < .5) THEN
    RCUT(1,2,3) = new value
    IWET = 0

↓

IF (IWET = 1) THEN
    RCUT(1,2,3) = new value

↓

IF (IWET > 1) THEN
    RCUT(1,2,3) = new value

END

SUBROUTINE ZENGEN

input: JDAY, TIME, LAT, LONG, ZONE
output: ZEN

subroutine in which the zenith angle is calculated.
the input-data needed for the calculation are: JDAY,
TIME (2400), LAT (latitude), LONG (longitude) and ZONE.

The zenith angle is used for the calculation of diffuse and direct components of the visible radiation and the sunlit and shaded leaf area.

SUBROUTINE WSTRESS

input: RG, AVSW, RAIN, TINT
output: FW

IF (RG < 10) THEN
    ET = 0
    FW = 1
    (ET = energy available for evaporation, FW is
    correctionfactor for waterstress)
    GO TO 10

ELSE
    calculation of ET and FW

10 calculation of ASVW using ET. ASVW is the available soil water in the upper 60 cm of the soil profile.

END

SUBROUTINE WNDPROF

input: USTAR, TLAI (LAITOT, LAI(L)),HC (HC(1), HC(L)), IPROF (IPROF(1), IPROF(L))
output: RB

subroutine that calculates the windprofile in the canopy
using a form of the exponential windprofile (Cionco)

↓

initialization of used parameters

↓

calculation of DO (displacement height) and ZO (roughness length) as a function of LAI based on computations of
Shaw and Pereira.

↓

calculation of U(21) (windspeed in upper layer)

↓

calculation of U(K) and RB(K) for every layer in the canopy.

↓

END

SUBROUTINE CANRAD2

input: PAI (MLAITOT, MLAI(1,L), ZEN, RG, FSL
output: RVD, RBVD

determination of the beam and diffuse components of the visible radiation (Norman and Weiss 1985).

↓

set fraction of total beam radiation and separate it into IR and visible components.

↓

computation of extinction coefficient.

↓

computation of the probability function for penetration of the beam component (Norman 1979).

↓

set the soil visible- and IR albedo

↓

computation of diffuse radiation penetration function and the ratio between R_{up} and R_{down}.

↓

initialization of downward diffuse components of visible radiation in the canopy.

↓

computation of downward radiation at each level and the upward diffuse fluxes using the soil albedo.

↓

start of iteration.

↓

computation of the upward diffuse fluxes for the visible wavelengths.

↓

check of iteration.

↓

END

SUBROUTINE TSTRESS

input: TMAX (TMAX(1,2), TMAX(L)), TMIN (TMIN(1,2), TMIN(L)), TOPT (TOPT(1,2), TOPT(L)), TA
output: FT

calculation of the correction factor for the cuticular resistance, dependent of temperature regime (TOPT, TMAX and TMIN)

SUBROUTINE CANRES

input: RSMIN (RSMIN(1,2), RSMIN(L)), B (B(1,2), B(L)), FT, FW, RC (RC(1,(1,2)), RC(L)), LAI(MLAI(1,(1,2)), MLAI(1,L)), RB, TA, RH

output:

computation of RS for sunlit and shaded leaves

DO FOR K=2 TO 21
    CALL FVDP → see SUBROUTINE FVDP
    calculation of RS for shaded leaves

    DO FOR I=1 TO 9
        CALL FVDP
        calculation of RS for leaves in the sun
END DO-loop

↓

computation of RC for each chemical species by correcting RC by the appropriate molecular diffusivities at 20 ^{0}C

RC=RS + RCUT + RMES (for the complete calculation see program)

↓

END

SUBROUTINE FVDP

input: VPLEAF, VPAIR (calculated in CANRES out of TA and RH), RB (RB(K)), RS (RSHADE(K), RSUN(K,I)
output: FV

calculation of the correction factor for RS, required because of a vapor pressure deficit.

Appendix C

Table of symbols

Symbols	Definition	Units
b'	response coefficient	$W\ m^{-2}$
c_v	constant (2.64 for $R_G > 75\ W\ m^{-2}$ and 2 for $R_G < 75\ W\ m^{-2}$	[-]
$f_{e,w,T,s}$	Correction factor for repectively humidity, water stress, temperature and molecular diffusivity	[-]
F_c	vertical flux of trace gas	$ppb\ m\ s^{-1}$
I_p	total diffuse and direct Photosynthetically Active Radiation	$W\ m^{-2}$
κ	von Karman constant (0.40)	[-]
L	Monin-Obukhov length	m
LAI	leaf area index	[ratio]
LAImax	maximum LAI	[ratio]
r_a	aerodynamic resistance	$s\ m^{-1}$
r_b	boundary layer resistance	$s\ m^{-1}$
r_c	canopy resistance	$s\ m^{-1}$
R_c	surface resistance	$s\ m^{-1}$
r_{cut}	cuticular resistance	$s\ m^{-1}$
r_{ctot}	integrated canopy resistance	$s\ m^{-1}$
r_{dead}	canopy resistance of dead vegetation	$s\ m^{-1}$
R_G	global radiation	$W\ m^{-2}$
R_{fol}	foliage resistance	$s\ m^{-1}$
r_i	intrinsic component of soil resistance	$s\ m^{-1}$
r_{mes}	mesophyl resistance	$s\ m^{-1}$
r_s	stomatal resistance	$s\ m^{-1}$
r_{smin}	minimal stomatal resistance	$s\ m^{-1}$
$r_{sl}(O_3)$	soil resistance (ozone)	$s\ m^{-1}$
r_u	near surface boundary layer component of soil resistance	$s\ m^{-1}$

T_a	absolute ambient air temperature	^0C
$T_{e,o,h}$	respectively characteristic minimal, optimum, maximum temperature	^0C
$\bar{u}$	average windspeed	$m\ s^{-1}$
u_*	friction velocity	$m\ s^{-1}$
$V_d(O_3)$	deposition velocity (ozone)	$cm\ s^{-1}$
V_d mod	model-derived V_d	$cm\ s^{-1}$
V_d corr	corrected measured V_d	$cm\ s^{-1}$
z	measurement height	m
z_0	roughness length for transfer of momentum	m
z_{0C}	roughness length for transfer of mass	m
σ_θ	standard deviation of the wind direction	rad 30 $minutes^{-1}$
Ψ_m	stability influence function for transfer of mass	[-]
Ψ_C	stability influence function for transfer of mass	[-]